



Norwegian University of
Science and Technology

Seismic Stratigraphic Interpretation of Late Palaeozoic Carbonates and Paleogeography of the Loppa High.

Heidi Vestly Holte

Petroleum Geosciences

Submission date: June 2016

Supervisor: Ståle Emil Johansen, IPT

Norwegian University of Science and Technology

Department of Petroleum Engineering and Applied Geophysics

Abstract

This thesis presents a detailed study of Late Palaeozoic stratigraphic successions on the Loppa High using seismic 2D and 3D data and well logs. Four intervals of interest have been mapped using carbonate stratigraphy methods. These intervals are highly affected by phases of tectonic activity on the Loppa High, which lasted from Devonian through Late Palaeozoic and into Triassic time. Climate change and extensive sea level change due to continental drift, tectonic activity and periodic icehouse conditions are the main controls on Late Palaeozoic carbonate successions on the Loppa High.

The oldest interval (Int1) is recognised as Carboniferous successions deposited in a tropical environment containing a mix of carbonate and siliciclastic sediments. The overlying interval (Int2) is recognised as a package consisting mainly of evaporite precipitation, which developed in a spill-out system during seasonal lowstands while the world experienced general icehouse conditions. The following interval (Int3), overlaying Int1 and Int2, is recognised as a Permian succession primarily consisting of carbonates. Carbonate build-ups are present near the south-western Loppa High, from the middle of the interval (Polarrev Formation) and are vertically extending to the top of the interval. The youngest interval (Int4) is a carbonate succession of Changhsingian age consisting of at least the mid-shelf carbonates of the Røye Formation.

Sammendrag

Denne oppgaven presenterer et detaljert studie av stratigrafiske avsetninger fra Loppahøyden under perioden Sen Paleozoikum. I kartleggingen er det brukt 2D og 3D seismisk data, og brønn data. Fire interessante intervaller har blitt kartlagt ved bruk av en stratigrafisk tolknings metodikk for karbonater. De kartlagte intervallene er sterkt påvirket av periodevis tektonisk aktivitet i området. Den tektoniske aktiviteten varte fra Devonsk tid, gjennom hele Sen Paleozoikum, og fortsatte inn i Trias. Avsetnings miljøet ved Loppahøyden i denne tidsperioden er sterkt påvirket av omfattende klima og havnivå endringer. Disse variasjonene kom av kontinentaldrift og periodiske istider.

Det eldste kartlagte intervallet (Int1) er en blanding av karbonater og silisiklastiske avsetninger fra Karbontiden, og er avsatt i et tropisk miljø. Det overliggende intervallet (Int2) er en sedimentpakke som primært består av evaporitter. Evaporittene kan ha blitt avsatt som «spill-out» systemer i under-bassenger på grunn av lavt havnivå i istid perioder. Det tredje intervallet (Int3) ligger over både Int1 og Int2, og består hovedsakelig av Permiske avsetninger. Karbonat oppbygninger er identifisert fra midten av intervallet (Polarrev formasjonen) og opptrer helt til toppen av intervallet. Det eldste intervallet (Int4) er avsatt i Changxing alder, og inneholder minimum Røye formasjonen. Denne er karakterisert som en midtre kontinental plate karbonat avsetning.

Acknowledgements

This thesis is the final project in the two year master program in Petroleum Geophysics at the department of Petroleum Engineering and Applied Geophysics, at the Norwegian University of Science and Technology (NTNU).

I would first and foremost like to sincerely thank my thesis advisor, Professor Ståle Emil Johansen (NTNU), for great support and guidance throughout the project. He has shown interest in the topic and helped steer me in the right direction during the progress of the project.

I would also like to thank PhD candidate Terje Solbakk (NTNU) for interesting discussions and insights regarding my thesis topic. He has shown enthusiasm for the project and many interesting discussions have given me a better understanding of the project topic.

Further I would like to acknowledge Dicky Harishidayat (NTNU) for always being available for technical support during this period and Doc. Kammaldeen Omosanya for good feedback with regards to the development of geological figures.

I would also like to give thanks to my fellow students at the computer room “GeoLab” at IPT, NTNU, for creating a good work atmosphere and for much laughter throughout the project period. Further I would like to give a special thanks to Marie Houge Nesheim and Richard Elks for reviewing this thesis.

Table of contents

1. Introduction.....	1
2. Regional setting of Loppa High.....	3
2.1 Geological setting of Loppa High	5
2.2 Late Palaeozoic setting of the western Barents Sea, with emphasis on Loppa High ..	7
2.2.1 Carboniferous.....	7
2.3 The effect of relative change in sea level and climate on carbonate development	9
2.3.1 Classification of carbonate depositional systems.....	11
3. Data and Method.....	13
3.1 Available seismic and wellbore data	13
3.2 Data Quality.....	15
3.3 Software used in the Study	16
3.3.1 Petrel.....	16
3.3.2 Adobe Illustrator	16
3.4 Carbonate stratigraphic analysis	17
3.4.1 The sequence stratigraphic method and terms	17
3.4.2 Seismic sequence analysis.....	18
4. Results and interpretations	21
4.1 Observations	21
4.1.1 Interval 1	25
4.1.2 Interval 2	27
4.1.3 Interval 3	29
4.1.4 Interval 4	31
4.2 Interpretation	33
4.2.1 Interval 1	34
4.2.2 Interval 2	34
4.2.3 Interval 3	35
4.2.4 Interval 4	36
5. Discussion	51
5.1 Paleogeography and sea level change on Late Palaeozoic Loppa High.....	51
5.1.1 Carboniferous	52
5.1.2 Permian.....	52
6. Conclusion	55

List of figures

Figure 2.1 Map showing the location of the study area.	3
Figure 2.2 Barents Sea lithostratigraphic chart.	4
Figure 2.3 Schematic illustration of the evolution of the North Atlantic and Arctic regions from Late Devonian to Triassic time.....	6
Figure 2.4 Carbonate classification and response to sea level change.....	12
Figure 3.1 Location of available data shown on a map of the study area.	14
Figure 3.2 Schematic view of some primary seismic reflection termination patterns, and their corresponding discontinuity surface.....	19
Figure 3.3 Schematic view of seismic reflection configurations.	19
Figure 4.1 Correlation between well sections	23
Figure 4.2 Correlation between wells, seismic and geological profile (GP).....	24
Figure 4.3 Time topographic map of the upper surface of interval 1.....	26
Figure 4.4 Time thickness map of interval 2.....	28
Figure 4.5 Time topographic map of the upper surface of interval 3.....	30
Figure 4.6 A time topographic map of the top surface of interval 4.	32
Figure 4.7 Location of geological profiles and seismic sections.	33
Figure 4.8 Geological profile 1.	38
Figure 4.10 Geological profile 2.	39
Figure 4.11 Geological profile 3.	40
Figure 4.11 Geological model 4.....	41
Figure 4.12 Geological profile 5.	42
Figure 4.13 Geological profile 6.	43
Figure 4.14 Geological profile 7.	44
Figure 4.15 Geological profile 8.	45
Figure 4.16 Geological profile 9.	46
Figure 4.17 Geological profile 10.	47
Figure 4.18 Geological profile 11.	48
Figure 4.19 Geological profile 12.	49
Figure 4.20 Facie map of Late Palaeozoic successions on Loppa High....	50

List of tables

Table 1 An overview of wells available in this project, with location shown on Figure 3.1... 13	
Table 2 an overview of main observations made on Late Palaeozoic successions on Loppa High. Based on well bore (Figure 4.1) and seismic data (Figure 4.8 – Figure 4.19).	22

1. Introduction

The Loppa High was formed as a structural high during Late Carboniferous rifting between Greenland and Norway. Older Carboniferous fault systems generally controlled the gradual eastward tilting of the Loppa High (Elvebakk et al., 2002, Rafaelsen et al., 2008). The tectonic faulting continued into Triassic time, and was dominated by extension and footwall uplift (Johansen et al., 1994). By the onset of Late Palaeozoic the climate on Loppa High was warm and humid, which created ideal conditions for carbonate development on the tilted ramp structure (Elvebakk et al., 2002).

Hydrocarbon exploration in the western Barents Sea started in the 1970s. In the 1980s, the three first exploration wells (7120/1-1, 7120/2-1 and 7121/1-1) penetrating Late Palaeozoic sediments on the Loppa High were drilled (Stemmerik and Worsley, 2005). The reservoir properties of the Late Palaeozoic western Barents Sea carbonates vary and are directly linked to paleo-climate and early secondary diagenetic processes in the form of dolomatization (Stemmerik and Worsley, 2005). However, the recent discoveries Alta (well 7220/11-1, 2014) and Gotha (well 7120/1-3, 2013) show promising reservoir properties in Permian carbonate successions. Carbonate successions have also been described from Bjørnøya and more recently from Svalbard as potentially good quality reservoirs. However, carbonate reservoir properties on the offshore Barents shelf are not well understood due to limited research and data (Stemmerik and Worsley, 2005, Sayago et al. 2012).

Ziegler (1982) has done much research on Late Palaeozoic paleogeography, however detailed studies on stratigraphy and paleogeography of Late Palaeozoic Loppa High development are still limited. As more than 40% of the worlds recoverable hydrocarbon in carbonate deposits have been trapped in stratigraphic unconformities, a detailed stratigraphic study is essential on the Loppa High carbonate deposits (Ford and Williams, 2013).

In this project seismic data and well logs will be used to study Late Palaeozoic carbonates on the Loppa High. By using seismic stratigraphic interpretation methods, a geological model will be created consisting of topographic maps and geological profiles. The geological model will be used to form a framework of Late Palaeozoic carbonates on the Loppa High. The frame work will contain detailed descriptions of Late Palaeozoic deposits, the location of the deposits and some interpretation of tectonism affecting the deposits. The detailed stratigraphic framework will then be discussed relative to the paleo-climate and paleo sea level in order to

get a greater understanding of the Late Palaeozoic paleogeography and the depositional environment of the Loppa High.

2. Regional setting of Loppa High

Loppa High is located in the Norwegian Barents Sea, north of Hammerfest Basin separated by the Asterias Fault Complex, east of Bjørnøya and Tromsø Basin separated by the Ringvassøy-Loppa Fault Complex, and south of the Bjarmeland Platform, as seen in Figure 2.1 (Gabrielsen et al., 1990). Loppa High is diamond shaped, and situated between 71°50'N, 20°E and 71°55'N, 22°40'E and 72°55'N, 24°10'E and 73°20'N, 23°E (Ahlborn et al., 2014, Gabrielsen, 1990). The Loppa High evolved as a structural high during Late Carboniferous rifting as a reaction to the Atlantic rift arm between Greenland and Norway (Figure 2.3). The eastward tilting of Loppa High was mainly controlled by older Carboniferous faults (Elvebakk et al. 2002). The Late Palaeozoic Loppa High is believed to have formed as a tilted carbonate ramp, due to the effects of tectonism, climate and eustatic sea level (Elvebakk et al., 2002, Rafaelsen et al., 2008). A lithostratigraphic chart is shown in Figure 2.2, displaying the general correlations between periods, ages, stratigraphic groups and lithological properties in specific areas in the western Barents Sea.

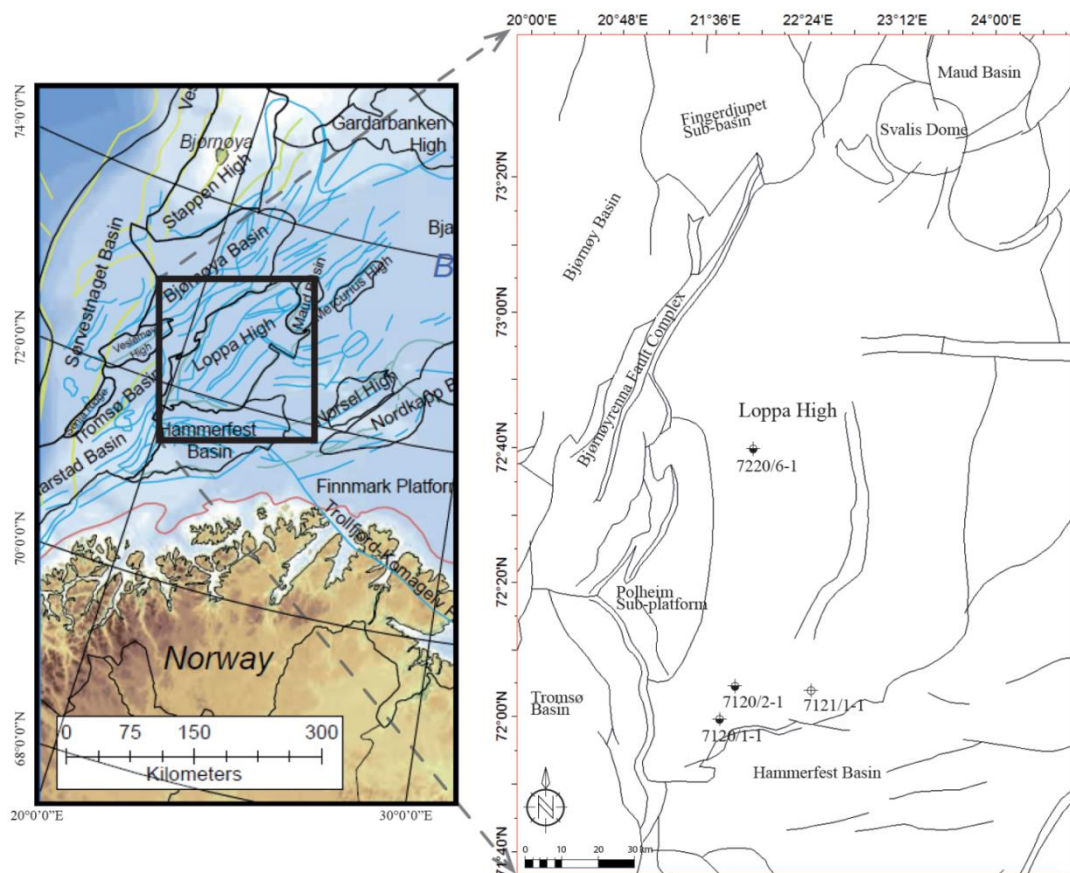


Figure 2.1 Map showing the location of the study area. Bathymetric map (left side) of the western Barents Sea, highlighting the study area by a black square. Map of the study area (right side). Modified from Di Lucia (2011) and Smelror (2009).

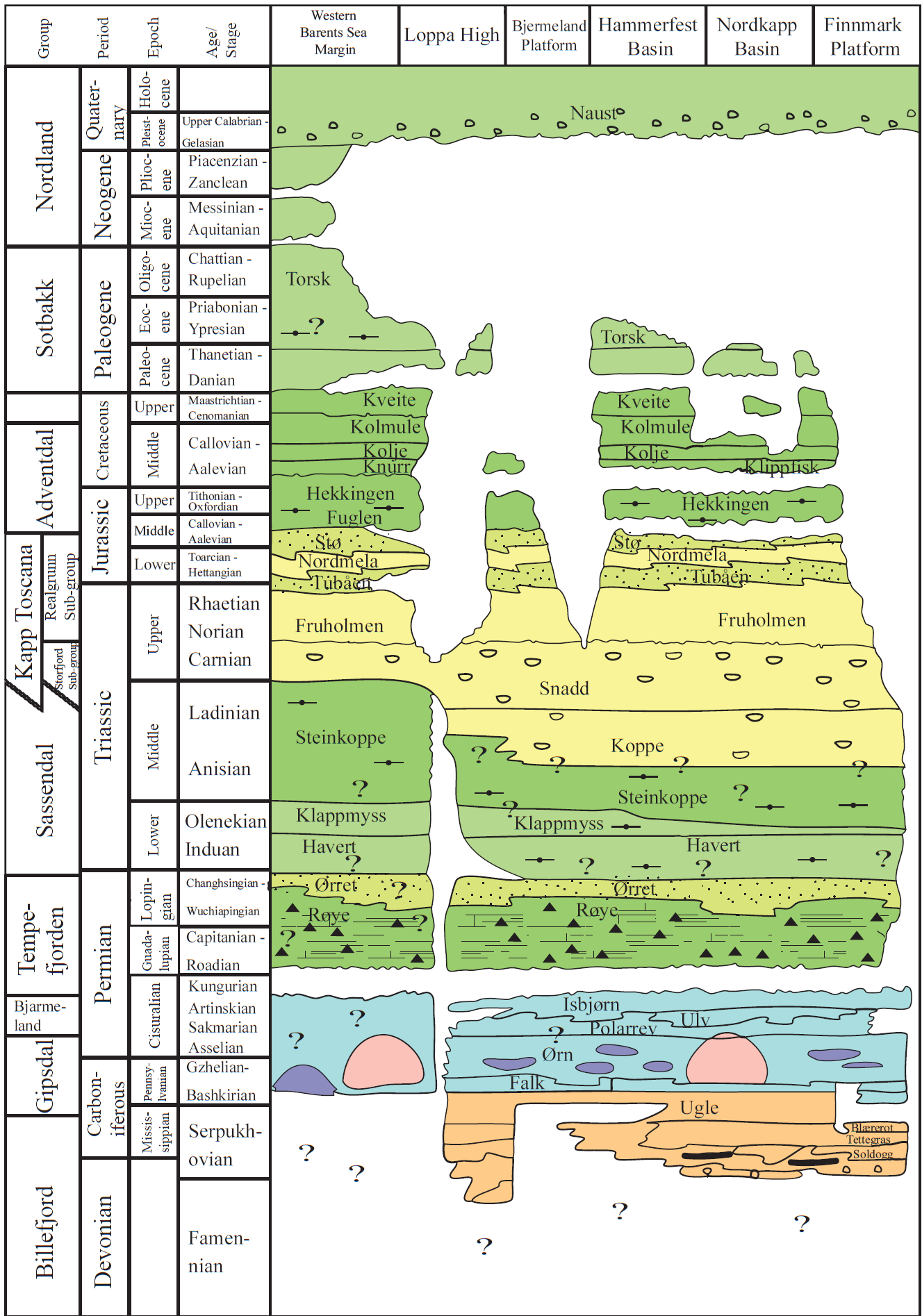


Figure 2.2 Barents Sea lithostratigraphic chart. Modified from NPD (2014).

2.1 Geological setting of Loppa High

At the onset of Late Palaeozoic time, the area from Arctic Canada in the west, across North Greenland and the Norwegian Barents Sea until Arctic Russia formed the east-west oriented northern margin of Pangea (Stemmerik and Worsley, 2005). The northern margin drifted northwards with a rate of about 2 mm/yr, from a paleo-latitude of approximately 20°N to 45°N during Carboniferous and Permian time (Figure 2.3) (Stemmerik and Worsley, 2005).

The western Barents Sea basement is believed to have consolidated during the forming of the Caledonian orogeny. The orogeny was developed in Norway through two major phases of tectonic regimes comprising both extensional and compressional events, lasting from (1) Late Cambrian – Early Ordovician and (2) Middle Silurian – Early Devonian (Gudlaugsson et al., 1998). The Caledonian orogeny is well documented from the exposed N–S striking bedrock which is exposed on the western coast of Spitsbergen (Smelror et al., 2009). The orogeny culminated in Early Devonian, and led to the merging of Laurentia and Baltica to become the so called “Old Red Continent”. Devonian tectonic regimes was followed by widespread rifting which controlled the western Barents Sea region in Late Palaeozoic, followed by non-fault related regional subsidence in Permian time (Gudlaugsson et al., 1998).

Post Caledonian rifting along the structure of the Caledonian Orogeny was accompanied by extensive sandstone erosion from the “Old Red Continent”. The erosion lasted from Devonian and into Early Carboniferous, creating accumulation of sandstone on the western Barents Sea shelf (Smelror et al., 2009).

The overlying Late Palaeozoic carbonate successions have experienced extensive dolomitization and dissolution of metastable carbonates during repeated subaerial exposure. Late Permian shallow water carbonates developed in cold climate are described by Stemmerik (1999) and Rafaelsen et al. (2008), as dominated by calcitic organisms and silica sponges, and as associated with calcite cement, mud and chert. The more recent Gotha discovery (well 7120/1-3) in 2013 and Alta discovery (well 7220/11-1) in 2014 shows promising potential in Permian carbonate reservoir on the high slope of Loppa High (Lundin Norway, 2016, NPD Fact Pages, 2016).

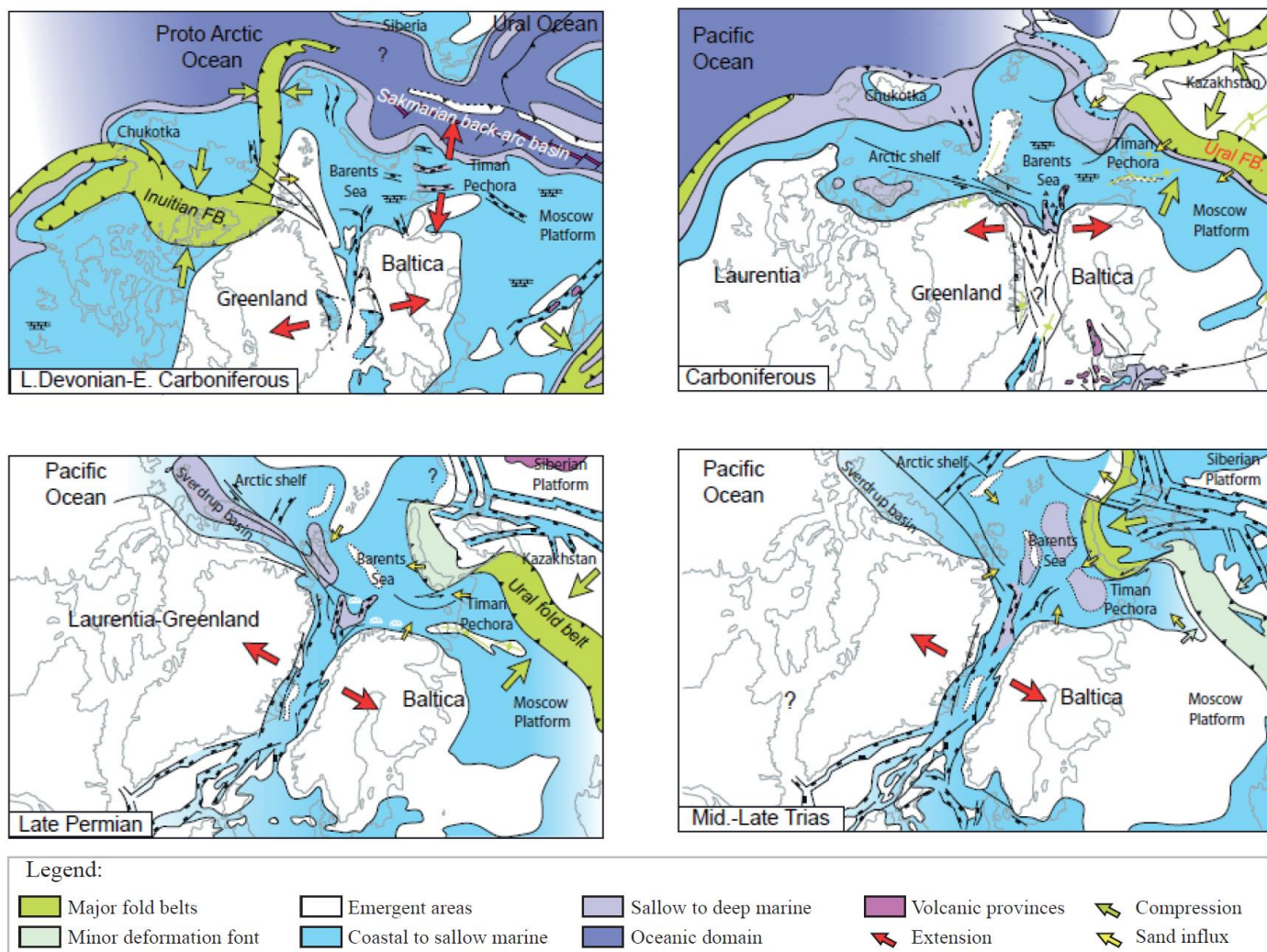


Figure 2.3 Schematic illustration of the evolution of the North Atlantic and Arctic regions from Late Devonian to Triassic time. From Smelror et al. (2009).

2.2 Late Palaeozoic setting of the western Barents Sea, with emphasis on Loppa High

The gradual shift in paleo-latitude of the western Barents Sea resulted in a climatic change from tropical and humid in Early Carboniferous, to temperate in Late Permian (Stemmerik and Worsley, 2005). Carbonate successions developed on the western Barents Sea during the Late Palaeozoic northwards movement of the Laurasian plate, from a location of around 25°N in Late Bashkirian (Late Carboniferous), to about 35-40°N by the Late Permian (Stemmerik et al., 1999).

2.2.1 Carboniferous

Regional extension dominated the landscape of the western Barents Sea during Carboniferous. The northern margin of Pangea developed two rift arms during Late Carboniferous, which divided large parts of the Barents Sea shelf into subsiding basins, and more stable platforms (Stemmerik and Worsley, 2005). These extension episodes were part of the long lived Palaeozoic – Mesozoic pre-opening rifting that would form the North Atlantic (Smelror et al., 2009).

During Viséan the climate was tropical humid in the western Barents Sea shelf, which was composed by a complex system of highlands, alluvial, fluvial plains, marshes and prograding deltas. The sedimentation was partly controlled by active horst – graben tectonics and basin development. Subsidence along basin margins was typical features affecting the Viséan environment. The Barents Sea landscape consisted of alluvial systems grading laterally into fluvial planes, lakes and marshes. The marsh deposits have normally been recorded as interbedded with coal and carbonate (Smelror et al., 2009).

2.2.2 Early Permian

The northern drift of the northern margin of Pangea resulted in a climatic shift from tropical humid to a semi-arid climate in Early Permian, on the entire Barents Sea shelf (Smelror et al., 2009). The Barents Sea was at the same time an object of regional transgression, which combined with the climatic change resulted in increased development of carbonate shelves, widespread evaporite depositions in deep marine basins, and also in shallow sabkhas (Smelror et al., 2009). Evaporite drilled in the Tromsø Basin has been dated to Late Carboniferous – Early Permian (Faleide et al., 1993).

During Moscovian to Early Sakmarian, carbonates developed in a warm water setting. The carbonates contain calcareous algae, mainly composed of aragonitic material and are associated with evaporites (Stemmerik et al., 1999).

The Asselian is generally an age associated with icehouse conditions and frequent and high amplitude eustatic sea level change, driven by glaciation on the southern hemisphere. However, warm water carbonates developed as extensive shallow marine carbonate shelves in the Barents Sea due to local warm conditions (Smelror et al., 2009). During episodes with high sea level, the entire shelf areas were flooded and shallow water carbonate platforms developed with up to 100 m thick build-up structures, also found on the Loppa High (Smelror et al., 2009). Halite deposition in basins took place during major low-stands when the structural highs were subaerially exposed, and the basins were entirely separated from the open ocean (Smelror et al., 2009). Carbon, oxygen and strontium isotope analysis from brachiopods sampled on Svalbard show distinct seasonal cyclicity of Early Permian paleo sea level (Nielsen et al., 2013).

During Late Sakmarian – Artinskian time, temperatures reduced and carbonates developed in cooler water, these deposits are recorded as mainly composed of calcite organisms and calcite cement (Stemmerik et al., 1999). The Barents Sea were in Artinskian – Roadian affected by an overall sea level change, and further in Kungurian – Roadian time successions of cold water carbonates developed with abundant chert in deep basinal areas (Stemmerik et al., 1999).

2.2.3 Late Permian

During Middle to Late Permian, tectonic tilting resulted in a subaerial exposure and erosion of the crest of Loppa High. The post deposited Bjermeland and Tempefjorden Groups was deposited as onlapping wedges (Elvebakk et al., 2002). The shift in climate during Late Permian led to temperate conditions and a gradual change from carbonate to a siliciclastic regime (Stemmerik and Worsley, 2005). There was a regional transgression during Wordian and a complex marine shelf with environments ranging from shallow to deep marine. The deep marine conditions, combined with the temperate climate in the western Barents Sea, led to ideal conditions for swamp colonies, which developed in the region. The main depositions in the western Barents Sea at the end of Permian consisted of chert, silicified carbonate, shales and siliciclastic sediments (Smelror et al., 2009).

2.2.4 Triassic

The Barents Sea was in Early Triassic affected by major rift episodes, followed by frequent transgression – regression variations, deltaic clastic sedimentation and a number of minor tectonic events (Smelror et al., 2009). Tectonic regimes on Bjørnøya and the Loppa High region were comprised by a series of minor uplift episodes (Smelror et al., 2009). Tectonic events in the Nordkapp Basin have been recognised as affected by salt movement from Early Scythian that lasted into Late Triassic (Smelror et al., 2009).

2.3 The effect of relative change in sea level and climate on carbonate development

There are four major variations that control the stratal patterns and lithofacies distribution of carbonate rocks: (1) Tectonic subsidence, which create space for the sedimentary deposits; (2) the volume of sediments, which controls paleo water depth; (3) eustatic change, which arguably have the largest control of carbonate production and stratal patterns; and (4) climate (Vail et al., 1984). (1) Tectonic subsidence is normally considered a slow change with respect to eustatic change (Sarg, 1988). (4) Climate includes rainfall and temperature, which is the major control of the type and distribution of both carbonate and evaporite deposition (Sarg, 1988). Evaporite deposition is also highly dependent on climate, and is often deposited associated with carbonate, primarily in arid environment, filling in shelf basins, lagoons, and supratidal flats (Sarg, 1988). The relative sea level rise creates the available space for sediment accommodation, and is an effect of tectonic change and primarily eustatic change (Sarg, 1988, Van Wagoner et al., 1990).

Carbonate develops are more or less in situ, within the depositional environment. Carbonate is mainly a by-product of photosynthesis as it primarily is produced of organisms (Schlager, 1981). Carbonate development is therefore dependent of light, and decreases with water depth. The development is most significant on a water depth of maximum 10 m, and drops significantly on in the interval between 10 and 20 m water depth. However, growth of carbonate has also been recorded in water depths between 50–100 m, where the environment still is sustainable for some organisms dependent of photosynthesis (Schlager, 1981, Sarg, 1988).

Carbonate reef development in the Bahama Banks and the Caribbean platforms, during the Holocene sea level rise illustrates the effect sea level change have on carbonate productivity (Schlager, 1981). The Holocene reefs were able to exceed the rate of sea level rise in the order of magnitude. The vertical growth is a function of total mass balance, limited by the relative rise in sea level. The maximum carbonate reef growth recorded on these Holocene successions had a rate of 12 000 to 15 000 $\mu\text{m}/\text{yr}$, and out-peaked the fastest sea level rise which reached about 8 000 $\mu\text{m}/\text{yr}$ (Macintyre et al., 1977). However, large areas of the carbonate platforms did not keep up the rate of the sea level change, which resulted in drowning of parts of the carbonate platforms (Schlager, 1981, Sarg, 1988). Most carbonate production is easily disturbed by sea level change, and also by other environmental change (Sarg, 1988).

There are three scenarios primary responses of carbonate depositions, when objected to a relative rise in sea level: (1) Carbonate build-ups and platforms can drown as a response to the rise in sea level. In this chase the shallow water deposition is often found underlying deep water sediments, or a condensed section (Kendall and Schlager, 1981); (2) only the fast growing rim or patched of the carbonate platform are able to keep up with the sea level rise, while the remaining carbonate platform drowns; (3) the carbonate platform is able to keep up with the sea level rise, which create a thickness that is at least equal to the height of the rise in sea level (Kendall and Schlager, 1981).

Relative drop in sea level cause karst and soil development over shelves or platforms, and are often accompanied by depositions of deep water evaporite in semi-enclosed basins and open marine basins (Kendall and Schlager, 1981). Evaporite deposits can occur as; an onlapping lowstand, or shelf margin wedge; a onlapping of retrogradational unit in the transgressional system tract; and as lagoonal/sabkhas in platform settings of the highstand system tract (Vail, 1987).

2.3.1 Classification of carbonate depositional systems

The accommodation of carbonate successions are closely related to relative change in sea level, and sea floor topography, as shown in Figure 2.4 (Carol et al., 2004, Schlager, 1991, Kendall et al., 1991). The close relation is due to the fact that carbonate production primarily is greater near the air/sea interface, as it is dependent on photosynthesis (Kendall et al., 1991, Sarg, 1988).

Sea level rise can result in five known outcome on carbonates development (Figure 2.4): (I) Give-up: carbonate production stops and the succession drown; (II) Back-step: production of basin margin carbonates stops, and the production repositions back across the shelf; (III) Catch-up: carbonate production is initially not able to keep the pace of sea level rise, but aggrades towards the sea level; (IV) Keep-up: carbonate production keeps the pace of sea level rise; (V) Prograde: carbonate production exceeds sea level rise, causing the platform margin to advance basinward (Kendall et al., 1991, Kendall and Schlager, 1981, Sarg, 1988).

Sea level fall will often result in termination of carbonate production due to a dry-up on the exposed shelf. While carbonate successions at the shelf margin and basinward can respond in three known outcomes: (1) Deep water slope and basin fan: the basin is still deep post to the sea level fall; (2) Shelf margin wedges: sea level fall create a basin shallow enough to maintain shallow water carbonate production of low-stand, keep-up and prograded wedges; (3) Spill-out: the sea level fall leads to isolation of a basin, and the local sea level rises due to depositional accumulation (shown in Figure 2.4 VI). The isolated water is then exposed in a larger area and gets evaporated faster. The carbonate production terminates and is replaced by evaporite precipitation (Kendall et al., 1991, Kendall and Schlager, 1981, Sarg, 1988).

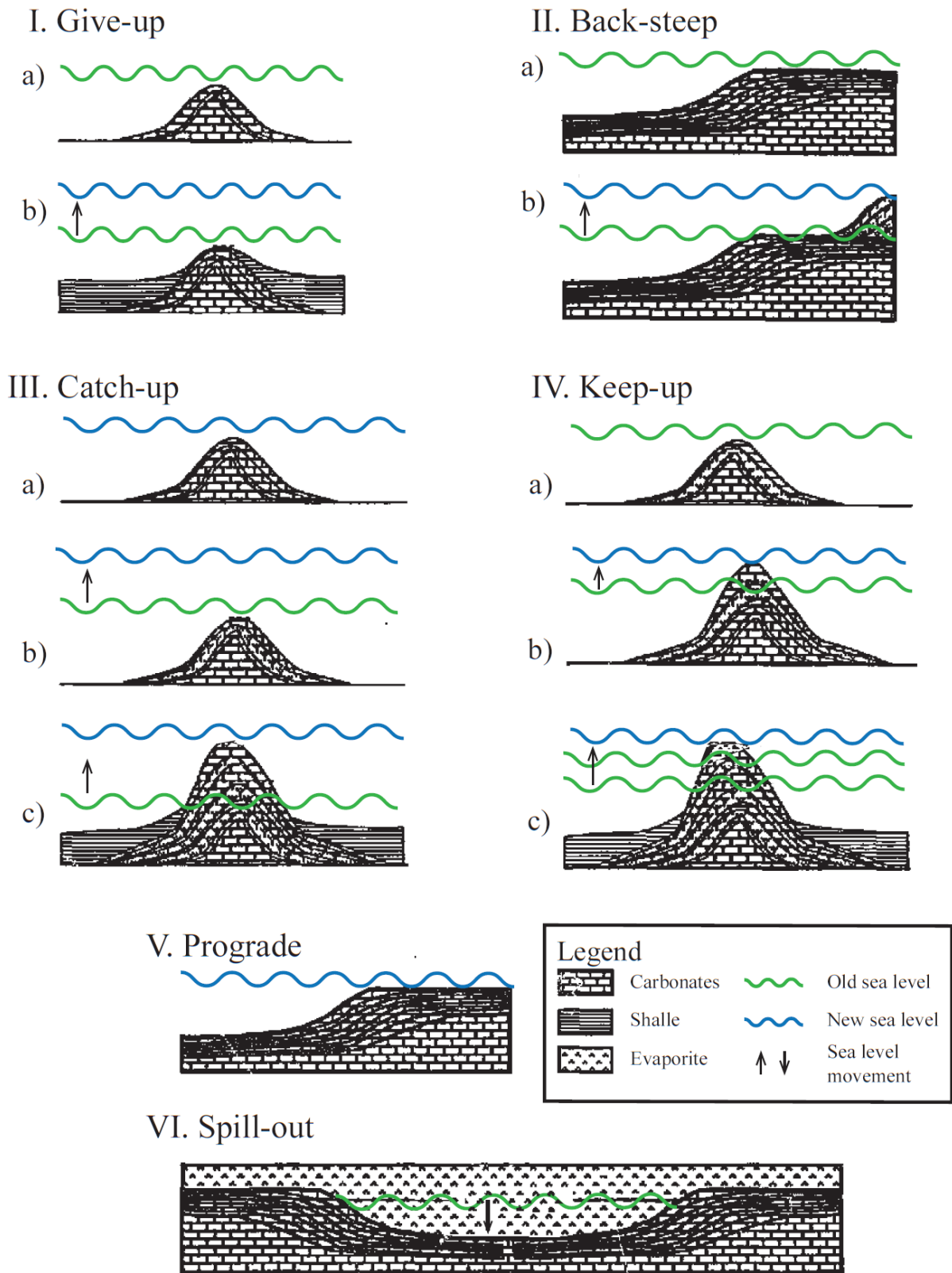


Figure 2.4 Carbonate classification and response to sea level change. Sea level rise can respond in, (I) Give-up: (a) Initial aggradation matches sea level rise. (b) rate of aggradation is less than rate of sea level rise, which leads to drowning and overlying deposition of shale or marls; (II) Back-steep: (a) Rapid carbonate accumulation prograde seawards. (b) Sea level rise exceeds carbonate production and carbonate production retreats (back-step) to a more favourable shallower position, and the carbonate again progrades; (III) Catch-up: (a) Sea level maintains a still stand, and the carbonate deposition catches up; (IV) Keep-up: (a) Initial aggradation matches sea level rise. (b) aggradation matches sea level rise. (c) carbonate aggradation matches rapid sea level rise; (V) Prograde: carbonate accumulates rapidly and area sheds downslope, and the succession grows seaward; (VI) Spill-out: Rapid sea level fall isolates the lowstand ocean water. Carbonate accumulates rapidly leading to a local sea level rise and a more widespread water area. The water is evaporated and precipitates evaporites. Modified from (Kendall et al., 1991).

3. Data and Method

3.1 Available seismic and wellbore data

The data used in this project consist of two-dimensional (2D) and three-dimensional (3D) zero phase seismic data made available through NTNU and Multi Client Geophysical Data (MCG), in addition to wellbore data, see Table 1. There are large variations in the quality of the seismic data. However, the MCG lines acquired from 2009, 2010 and 2012 are of high quality and have been interpreted with the highest confidence. Therefore these lines has been used as a reference, and tied to the lower quality data in order to get a high confidence interpretation.

The visible variations in seismic response within one single seismic section, is often variations due to velocity anisotropy. This means that the seismic pulse has a longer travel time when propagating through some lithological packages than other (Herron and Latimer, 2011).

Table 1 An overview of wells available in this project, with locations of the wells shown on Figure 3.1.

	<i>Wellbore name</i>	<i>Discovery</i>	<i>Oldest penetrated age, Formation</i>	<i>Year drilled</i>
Wellbore data	7120/1-1	No	Late Permian, Ørret Formation	1985
	7120/2-1	No	Indeterminate, Basement	1985
	7121/1-1 R	No	Late Carboniferous, Ørn Formation	1986
	7220/6-1 (Obelix)	No	Pre-Devonian, Basement	2005

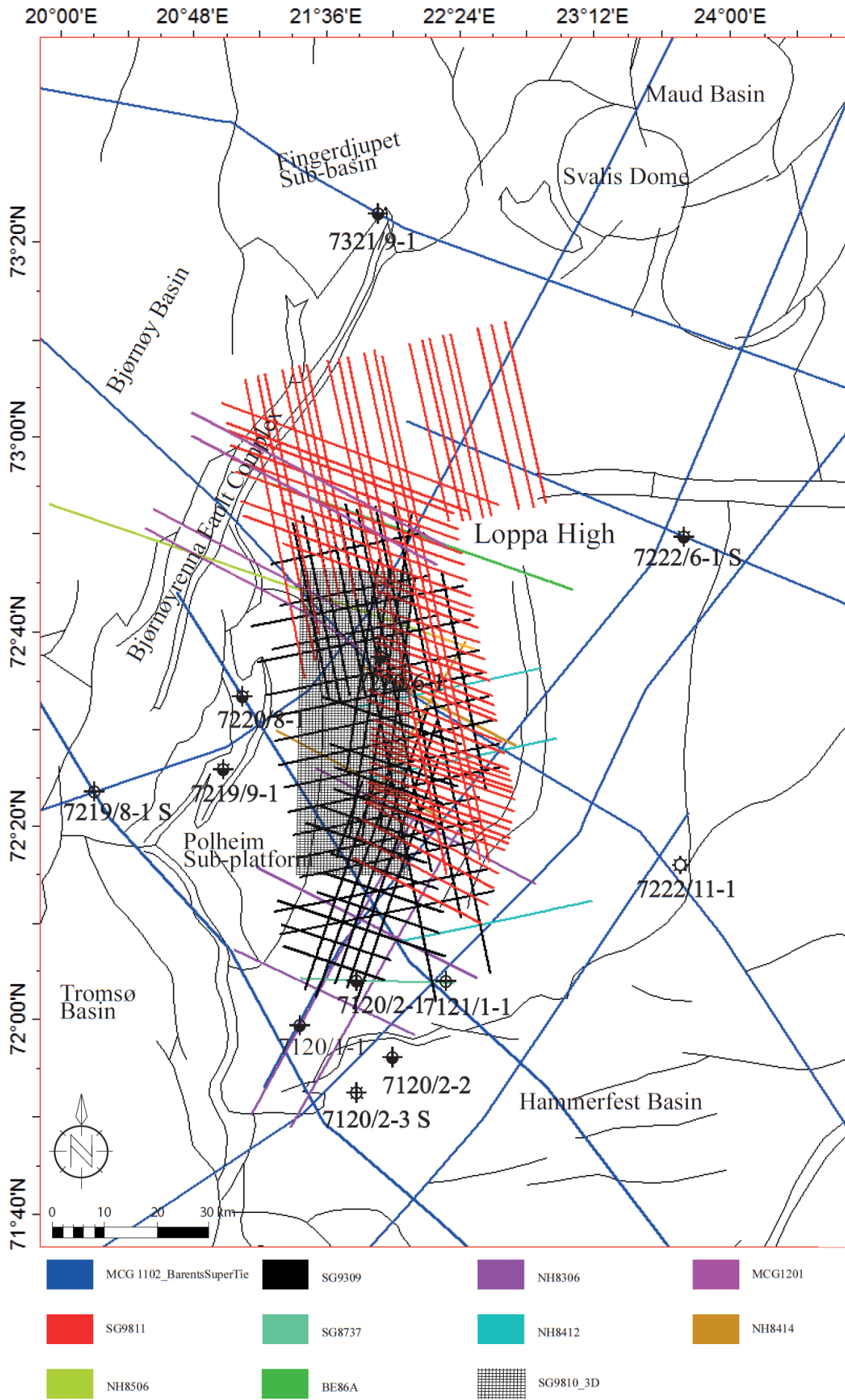


Figure 3.1 Location of available data shown on a map of the study area. An overview of the available wells used in this project are shown in Table 1.

3.2 Data Quality

Quality is defined as the degree of which something fulfil its intended purpose, the quality of seismic data is therefore dependent on the resolution, and thereby its ability to distinguish between different geological packages (Herron and Latimer, 2011).

The vertical resolution is limited by $\lambda/4$, where λ is the wavelength (Sheriff and Geldard, 1995). This limit was defined by Lord Reyleigh in the 19th century, and means that packages with a greater thickness, thicker than $\lambda/4$, will be visible on seismic sections with a top and base reflection. Packages thinner then this limit ($\lambda/4$) will be visible only as one strong reflection. The ability to distinguish between different packages is therefore given by the formulas (Landrø, 2011):

$$\text{Vertical resolution} = \frac{\text{Wavelength}}{4} \quad (1)$$

$$\text{Wavelength} = \frac{\text{Velocity}}{\text{Frequency}} \quad (2)$$

With increased depth in the seismic data, the velocity increases and the frequency decreases, which results in an increase of wavelength, and a decrease in vertical resolution (Boggs, 2010).

The horizontal resolution is recognized as the first Fresnel zone, which is defined as the area where the reflected energy arrives at a detector, and has phases which differentiate with maximum a half-cycle (Sheriff and Geldart, 1995). The radius of the first Fresnel zone is given by:

$$R_1 = \sqrt{\frac{\lambda h_0}{2}} = \frac{v}{2} \sqrt{\frac{t}{f}} \quad (3)$$

where h_0 is the depth, v is average velocity, t is two way travel time, and f is frequency. The relationship between frequency and horizontal resolution is similar to the vertical resolution, where high frequency equals high resolution (Bogg, 2010, Sheriff and Geldart, 1995).

3.3 Software used in the Study

3.3.1 Petrel

The Schlumberger software Petrel is the main software used in this project. Petrel has been used for visualizing and interpretation of 2D and 3D seismic data as well as for wellbore data. The seismic visualization has mainly been displayed in seismic default colours, with a vertical exaggeration (VE) of 1:5. The well data (for wells defined in Table 1) have been tied to the seismic data by performing forward modelling on a synthetic seismogram that were developed using the sonic and density logs.

The “make horizon” function was used to make detailed interpretations of the main seismic intervals in the study. However, 2D seismic data limits the detailed interpretation, as there are large areas with no available data between the sections (Figure 3.1). The “ghost” function was used to compare and look for similarities between seismic sections at difficult areas, in order to get a more accurate interpretation. The RMS- attribute has also been used in order to differentiate some high and low amplitude seismic patterns. The “make surface” function was used on the interpreted horizons, and converted the horizons into continuous surfaces. The “make surface” function create a linear function between interpretations if there are uninterpreted areas (for example between 2D seismic sections, as can be seen in Figure 3.1). The linear function creates some uncertainty in the maps created from the surfaces. The “create thickness map” function has been used to illustrate the two way travel-time (TWT) thickness of a specific seismic package. Polygons surrounding the surfaces and maps have been used to calculate the area of each interval, and the “Petrel measuring devise” have been used to obtain width and thicknesses of specific features within the seismic sections.

3.3.2 Adobe Illustrator

Adobe Illustrator was used to create geological profiles based on seismic sections. Maps originally created in Petrel was exported and further adjusted in Adobe Illustrator. These adjustments were due to limited data in specific areas (Figure 3.1), and the adjusted was based on literature studies.

3.4 Carbonate stratigraphic analysis

Vail (1987) and Van Wagoner et al. (1990) described the method sequence stratigraphy as the framework of an ideal sequence, consuming specific units, or “building blocks”. The method carbonate sequence stratigraphy was later specified by Sarg (1988). In this project these methods will be attempted in order to create a stratigraphic framework of Late Palaeozoic carbonate successions on the Loppa High. In order to avoid confusion between the ideal sequence, and the main stratigraphic packages recognized in this project, the main packages will be described using the term intervals (Vail, 1987, Van Wagoner et al. 1990). An interval will in this project describe a package containing similar properties within the seismic and well data. The intervals have further been analysed and interpreted based on stacking and termination patterns.

3.4.1 The sequence stratigraphic method and terms

The stratigraphic sequence is formed by three system tracts, where each system tract represents a contemporary depositional system (Van Wagoner et al., 1990). The different system tracts are shelf margin (SMST); lowstand (LST); transgressive (TST); and highstand system tracts (HST) (Elvebakk et al., 2002, Posamentier, 1988, Vail, 1987, Van Wagoner et al. 1990).

The system tracts contain one of the three specific stacking pattern described by Vail (1987) and Van Wagoner et al. (1990), and are dependent on the relationship between rate of deposition, and rate of acquired accommodation space. (1) The progradational stacking pattern is recognised by sediments building basinward. It is primarily related to a slow rise in sea level, where the rate of deposition exceeds the rate of acquired accommodation space (Holte, 2016, Sarg, 1988, Van Wagoner et al., 1990). (2) The retrogradational stacking pattern is recognised by a back-stepping depositional trend. It is generally associated with a relative sea level rise, and is the result of a rate of deposition slower than the rate of acquired accommodation space (Holte, 2016, Sarg, 1988, Van Wagoner et al., 1990). The aggradational stacking pattern can be recognised by a vertical depositional build-up trend. It is associated to a stationary or slow rise in sea level, and is an effect of an approximately equal rate of deposition and rate of accommodation space (Holte, 2016, Sarg, 1988, Van Wagoner et al., 1990).

The SMST is a progradational to aggradational wedge overlying a type 2 sequence boundary, and laps out on the platform, landwards of the platform or bank margin. The underlying type 2 sequence boundary is a conformable boundary affected by subaerial exposure of the inner-platform, and the upper boundary is a transgressive surface (Sarg, 1988, Van Wagoner et al., 1990).

The LST is deposited basinward from the platform or bank margin, overlying a sequence boundary. The LST laps out on, or near the platform margin and fills incised valleys associated with the underlying type 1 sequence boundary. The upper boundary of both the LST and the SMST is the transgressive surface (Sarg, 1988, Van Wagoner et al., 1990).

The TST consists of a retrogradational pattern, which thickens towards the shelf, until it thins out and onlaps in more distal locations basinward. The younger depositions are in general progressively thinner as a result of sediment starvation. The deposition is followed by the forming of a condensed section, or maximum flooding surface (mfs), which represents the upper boundary of the TST (Sarg, 1988, Van Wagoner et al., 1990).

The HST represents the final package of the sequence, and can be recognised by a prograding to aggrading stacking pattern, often forming a sigmoidian to oblique clinoform. The lower boundary of the HST is a downlap surface associated with the maximum flooding surface. The upper surface of the HST is the sequence boundary (Sarg, 1988, Van Wagoner et al., 1990).

3.4.2 Seismic sequence analysis

An under group of sequence stratigraphy is the method seismic sequence analyses described by Vail (1987), which analyses the discontinuities and terminations of seismic reflections, shown in Figure 3.2. The method will be attempted in order to understand the seismic stratigraphy, by recognising converging seismic reflections and interpret the discontinuity and termination patterns.

There are two types of termination patterns that laps out above the discontinuity: the onlap pattern; and the downlap pattern (Figure 3.2). (1) A regional onlap overlying a truncation is normally interpreted as a sequence boundary. Onlaps can also be helpful characteristics when interpreting mounding, channel deposits and slope deposits. (2) Regional downlap characteristics are likely to create a downlap surface, which can represent: a top basin flood fan surface; top slope fan surface; or a maximum flooding surface (Vail, 1987).

There are three types of reflection terminations that lap out below the discontinuity: truncation; (1) toplap (2); and apparent termination (3). (1) Truncations are associated with an eroded surface (Mitchum Jr et al., 1977). (2) Climbing toplap is often a good indication of deep marine current deposits. (3) The apparent truncation and downlap patterns are often associated with sediment starvation Figure 3.2 (Vail, 1987).

Discontinuities and terminations

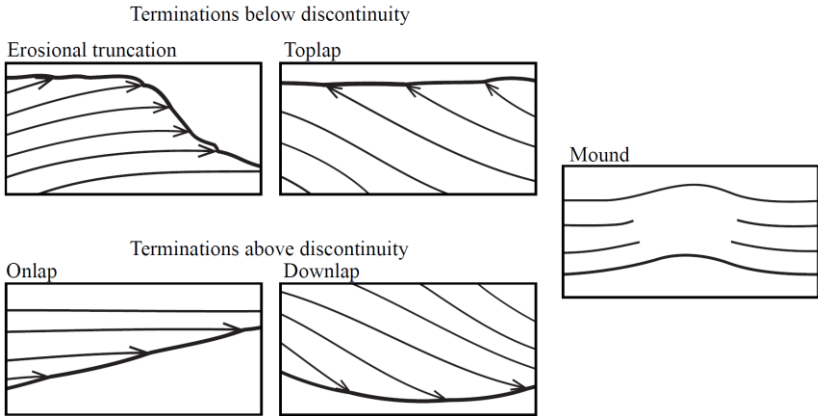


Figure 3.2 Schematic view of primary seismic reflection termination patterns, and their corresponding discontinuity surface. Modified from (Mitchum Jr et al., 1977).

Seismic reflection configuration will be used to distinguish between seismic intervals, as described by Bubb and Hatlelid (1978). The visual differences in seismic reflection properties are continuity, amplitude and frequency, shown in Figure 3.3.

Reflection configuration

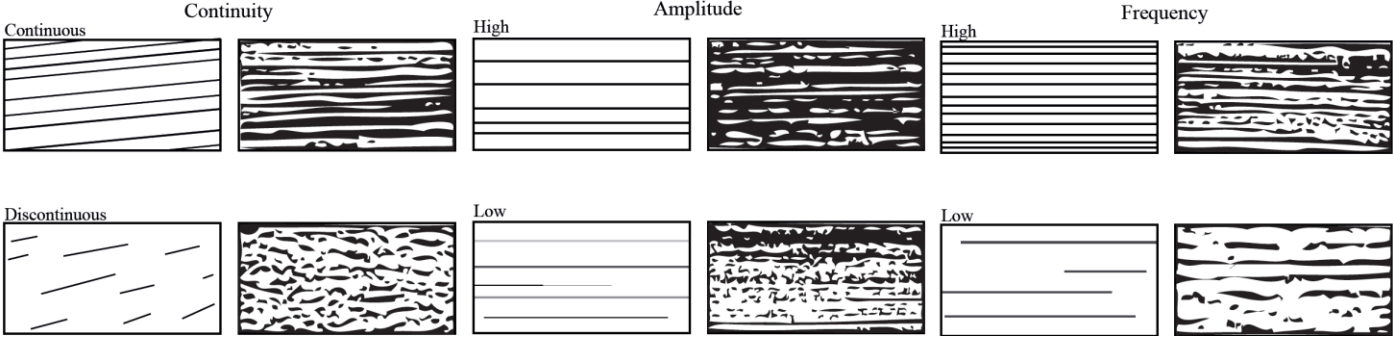


Figure 3.3 Schematic view of seismic reflection configurations.

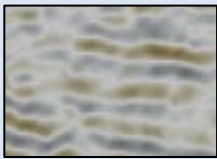

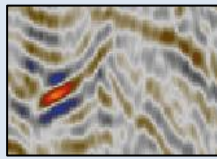
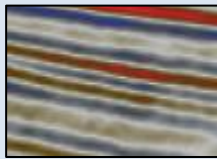
4. Results and interpretations

4.1 Observations

In this study, the observations are focused on trends in seismic reflection configurations, stacking patterns and reflector terminations as well as in gamma ray (GR) and sonic log (DT) responses. The observations in the Late Palaeozoic successions are describing chronologically from the lowermost interval 1 (Int1) to the uppermost interval 4 (Int4). The primary observations made from well logs and seismic data are summed up in Table 2.

Four wells available for this study penetrate the Late Palaeozoic successions on the Loppa High. The wells 7120/1-1; 7120/2-1; 7121/1-1 R; and 7220/6-1 are shown with well sections and locations on Figure 4.1. Three intervals of Late Palaeozoic age, with slight differences in well log responses have been identified, and highlighted with black squares in Figure 4.1. None of these four wells have been cored in the Late Palaeozoic successions. The four wells available for this study has been tied to the seismic data as shown in Figure 4.2.

Table 2 An overview of main observations made on Late Palaeozoic successions on Loppa High. Based on well bore data (Figure 4.1) and seismic data (Figure 4.8 – Figure 4.19).

Intervals:	<i>Interval I</i>	<i>Interval II</i>	<i>Interval III</i>	<i>Interval IV</i>
Gamma ray (GR) response	Low but uneven, with many peaks	Not present	Low	Low
Sonic response (DT)	Low, some peaks	Not present	Low	Low – medium
Amplitude	Low	High	Low	Medium-high
Frequency	Low	Low	High	High
Continuity	Low	Medium	Low to medium	High
Mound	No	No	Yes	Some
Termination / discontinuity	Eroded on the western edge	Onlapping (area A, downlapping and truncation)	Onlapping, truncated on the western edge	Onlap and truncation (some offlap trends)
Stacking pattern	Aggradational and progradational	Aggradational	Progradational to aggradational	Aggradational to retrogradational
Maximum thickness (approximation)	440 ms	400 ms	400 ms	200 ms
Area (approximation)	$1.8 \times 10^{10} \text{ m}^2$	$6.9 \times 10^9 \text{ m}^2$	$1.6 \times 10^{10} \text{ m}^2$	$1.4 \times 10^{10} \text{ m}^2$
Example (Vertical 150 ms, horizontal 750 m)				

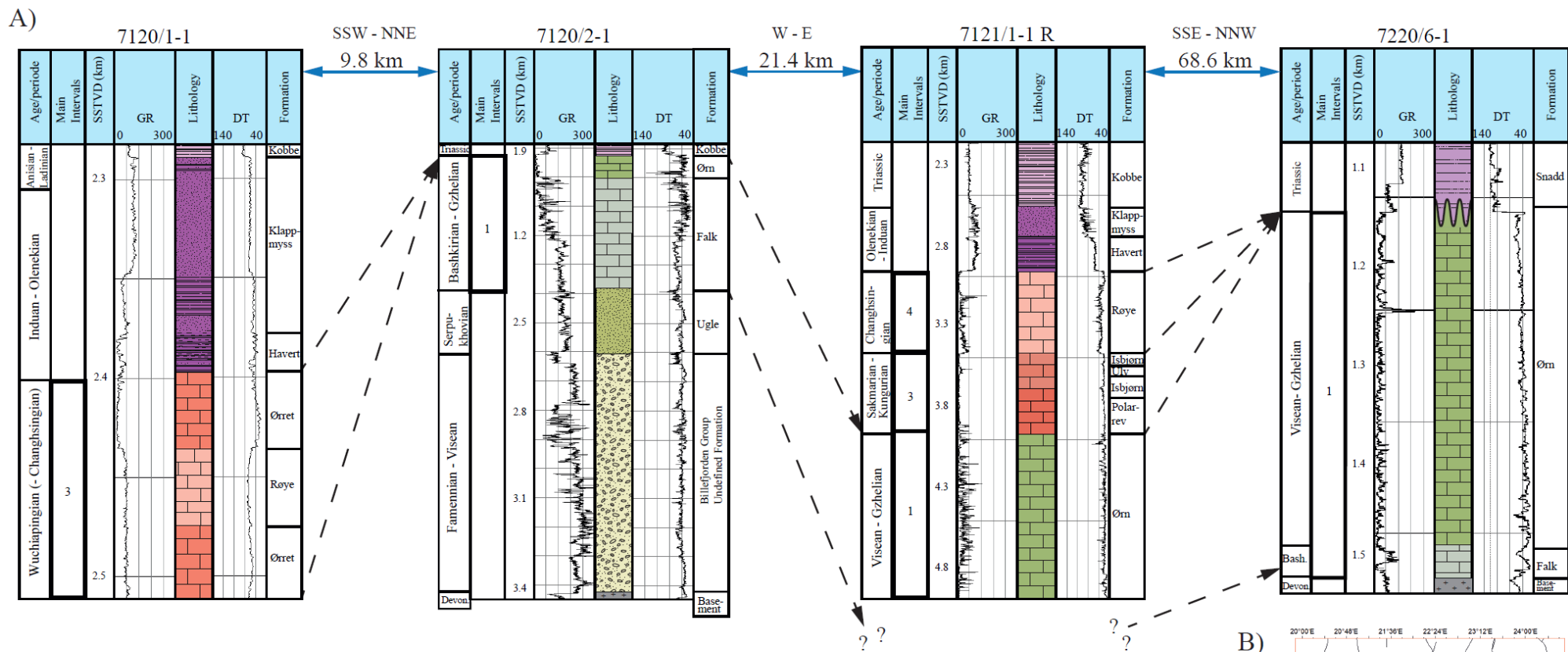
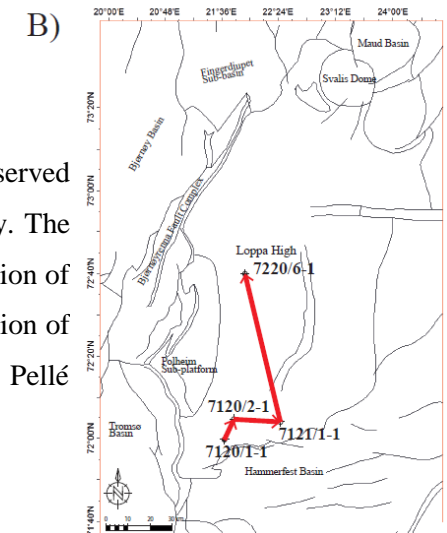


Figure 4.1 A) Correlation between well sections of the wells 7120/1-1, 7120/2-1, 7121/1-1 R and 7220/6-1. The main intervals observed are highlighted with black squares and are correlated to age or period, depth, gamma ray log (GR), sonic log (DT) and lithology. The intervals are also correlated between the wells by black arrows. The entire interval 1 may be present with parts below the well section of well 7121/1-1 R and is marked by question marks. B) The well location is shown in map view with red arrows showing the direction of well section from left to right. Standard colour codes for the geological time scale are used on the lithology, composed by J.M. Pellé (CGMW, 2012).



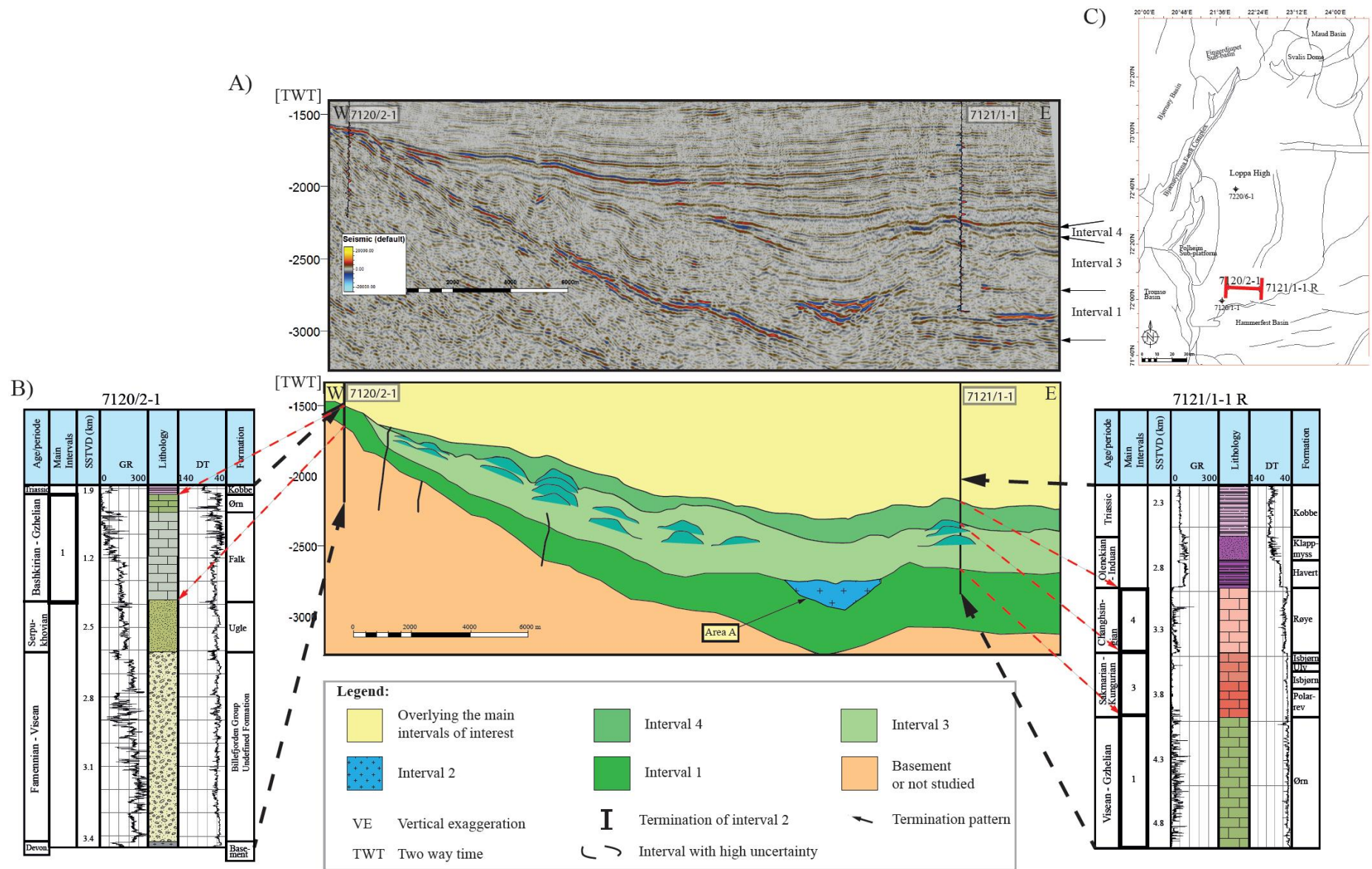


Figure 4.2 Correlation between wells, seismic and geological profile (GP). The vertical extension used in the seismic and in the GP is 1:5. A) The seismic section SG8783-102, with wells displayed with synthetic seismograms, illustrates a good tie between wells and seismic. B) The well sections of wells 7120/2-1 and 7121/1-1 R have been correlated to the GP based on the well section. Black arrows correlate between the well sections and the well area in the GP, red arrows correlate the main intervals between the well section and the GP. C) Map of the study area, with a red line highlighting the location of the seismic section. The legend also corresponds to Figure 4.8 to Figure 4.19.

4.1.1 Interval 1

The lowermost interval, Int1, is observed in wells 7120/2-1, 7121/1-1 R and 7220/6-1, and is characterized by generally low GR and DT responses (Figure 4.1). The GR response is increasing with depth in well 7120/2-1, and is somewhat uneven with peaks observed in all of the three well sections. DT is also showing some irregularities with small peaks. The largest irregularities observed in the well logs, are found in well 7120/2-1.

Int1 is from the seismic sections characterized by low amplitude, low frequency and chaotic seismic patterns (see seismic sections in Figure 4.8, Figure 4.10 and Figure 4.14). Int1 is in some areas difficult to differentiate from the slightly higher amplitude and continues underlying unit (Figure 4.14). In specific areas where Int1 is underlying Int2, there is an abrupt increase in amplitude of Int1 (see seismic sections shown in Figure 4.9, Figure 4.11, Figure 4.14 and Figure 4.18).

The interval is observed in large parts of the Loppa High, and is thinning towards the most elevated region close to the Bjørnøyrenna Fault Complex on the western edge of Loppa High. Int1 is observed as an aggradational to progradational package, which onlaps the underlying units. The depth in TWT to the top surface of Int1 is shown by the topographic map shown in Figure 4.3. The surface is shallowest near the western Loppa High and towards the Svalis Dome. The surface deepens towards the east and south-east, and has an abrupt deepening into the Hammerfest Basin. The interval terminates by onlap against the western margin of Loppa High.

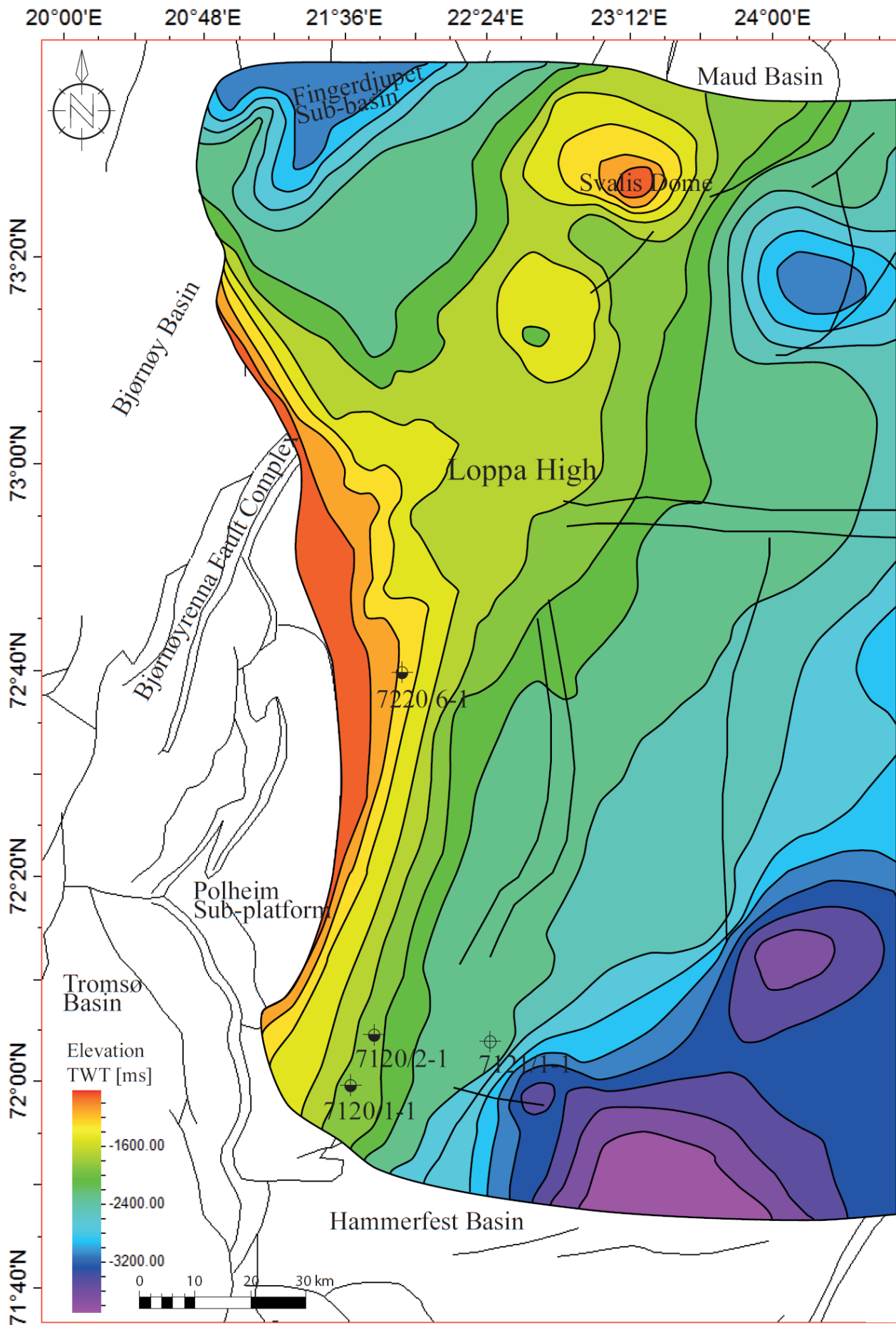


Figure 4.3 Time topographic map of the upper surface of interval 1. The surface is further shown as the upper boundary of interval 1 in Figure 4.8 - Figure 4.19.

4.1.2 Interval 2

Interval 2, Int2, is overlying Int1, and is characterized by very high amplitude, low frequency and chaotic seismic patterns. The interval has not been recognized in well data (Figure 2.1), and is only found in 2D seismic sections on the deeper central and eastern Loppa High. From the time thickness map seen in Figure 4.4, Int2 is not located at the well positions. Int2 is found as four isolated units which will be described further as area A, B, C and D (Figure 4.4). The seismic reflections patterns of Int2 are terminating as downlapping and onlapping onto the discontinuity surface of top Int1, they are also found as truncated to the discontinuity surface of base interval 3 (Int3).

Area A is the largest unit of Int2, located in the central to south-eastern Loppa High (Figure 4.4). The area is overlying the deepest parts of the top surface of Int1 on the Loppa High. Area A are terminating by truncation in the north, continuing in the east and until the south-west (see seismic section in Figure 4.17 and Figure 4.19). In the north-west close to area B, area A is containing onlap and downlap patterns (see seismic section in Figure 4.9, Figure 4.13 and Figure 4.15).

Area B is a hammer shaped unit located on the northern Loppa High. The main termination trend of the area is onlap to Int1 (see seismic section in Figure 4.9, Figure 4.13 and Figure 4.14), some downlap in the very north and south (see seismic section in Figure 4.10), and truncation in the west (see seismic section in Figure 4.11).

Area C is located near the north-western margin of Loppa High. The area is generally terminating by onlap (see seismic section in Figure 4.11 and Figure 4.14), with some truncation on the southern edge (see seismic section in Figure 4.12).

Area D contains many similar characteristics as area A, B and C, high amplitude, low frequency and overlying Int1 (see seismic section in Figure 4.8). Area D is located outside Loppa High, on the southern margin of the Fingerdjupet Sub-Basin (Figure 4.4). The area contains somewhat more continues seismic pattern (see seismic section in Figure 4.8), and is not found on any seismic sections where area A, B or C are also present. Area D is therefore considered a high uncertainty area (marked with question marks on Figure 4.4), and is regarded as not of main interest in this project.

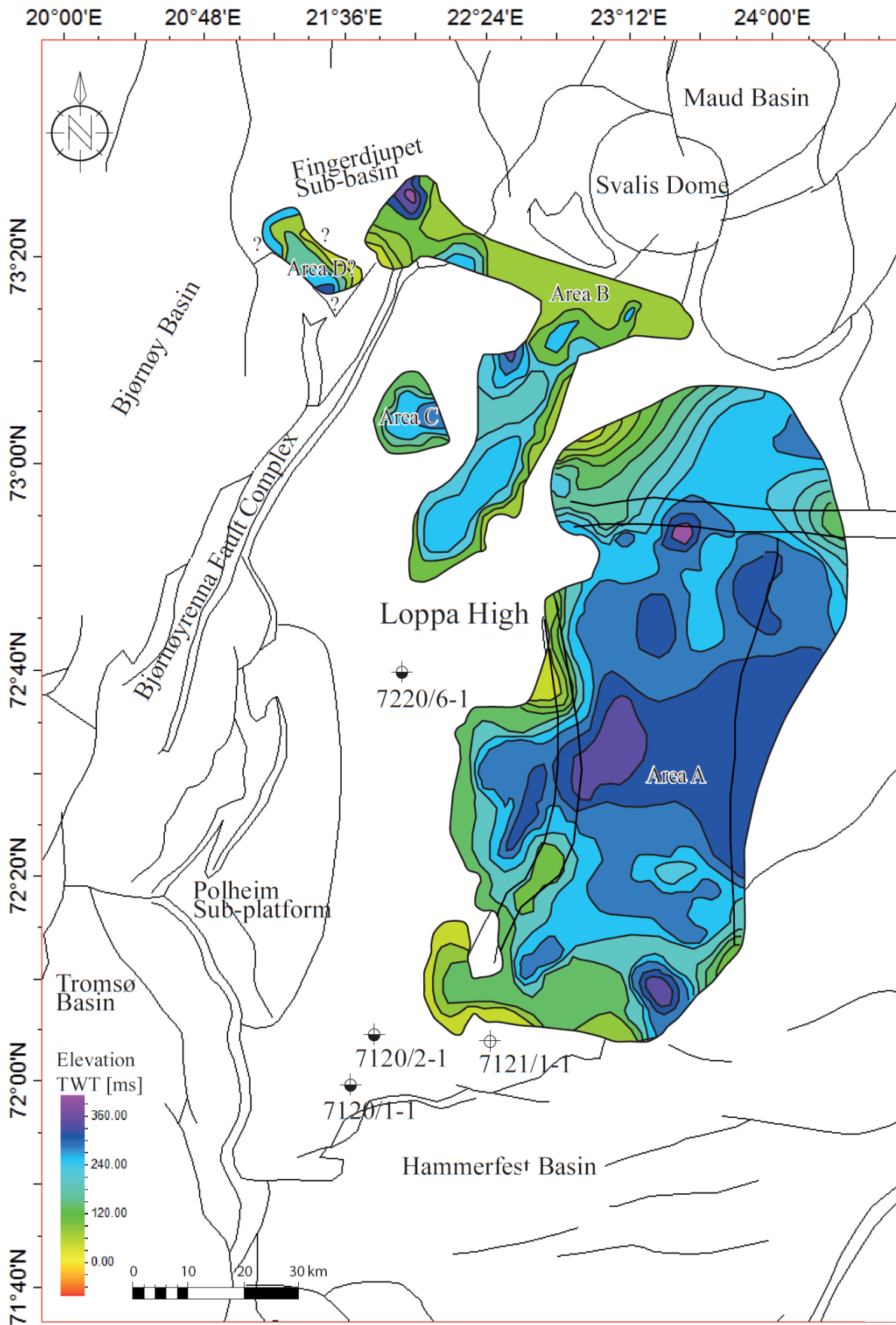


Figure 4.4 Time thickness map of interval 2. Showing the location of the four separate areas of interval 2; area A; B; C; and D. Area D is marked with question marks and is regarded as a high uncertainty area and is not of main interest. Interval 2 is shown on seismic cross sections in Figure 4.8 - Figure 4.19.

4.1.3 Interval 3

Int3 is observed in well 7120/1-1 and 7121/1-1 R, and shows many characterizations similar to Int1 (Figure 4.1). However, Int3 shows an overall smoother log pattern on both the GR and the DT log, with higher values in the lower part on the logs of well 7120/1-1. There is also observed slightly higher values and small peaks in both GR and DT on the intersection between Int1 and Int3 in well 7121/1-1 R. In well 7120/1-1 the lower part of Int3 has an increase in both GR and DT. Int3 has a wide age span and consists from the logs of the Polarrev-, Isbjørn, Ulv, Ørret and partly Røye Formations.

Int3 is overlying Int1 in the well section of well 7121/1-1 R (Figure 4.1). However, from seismic sections (seen in Figure 4.8 - Figure 4.19), Int3 is overlying Int1 in the shallower areas near the margins of Loppa High, and as overlying Int2 in the majority of the Loppa High region.

Int3 is characterized by partly continues, low amplitude and high frequency seismic patterns (see seismic section in Figure 4.9, Figure 4.11 and Figure 4.12). It is generally progradational to aggradational, and onlapping the underlying intervals. The time topographic map of the top surface of Int3 is shown in Figure 4.5, and characterises similar topographic trend as Int1. The shallowest part of the interval is located near Loppa High and towards the Svalis Dome, and deepening to the east and south east. The interval is terminating by onlap onto the top surface of Int1 near the western margin of Loppa High.

In the shallow areas near the west and north-western margin, the interval contains mounding reflections with aggradational stacking patterns from the middle part of Int3 until the top of the interval. The largest mounding reflection of Int3 is recognised in the 3D seismic survey located in in the south-western Loppa High (3D seismic shown in Figure 3.1 and build-up locations on Figure 4.20). The upper parts of the mounding reflections are in primarily shallower than the surrounding surface of top Int3 (see seismic section of Figure 4.12 and Figure 4.18). The interval is in the north-west highly affected by faults (see seismic section of Figure 4.11 and Figure 4.14), making it difficult to distinguish mounding patterns.

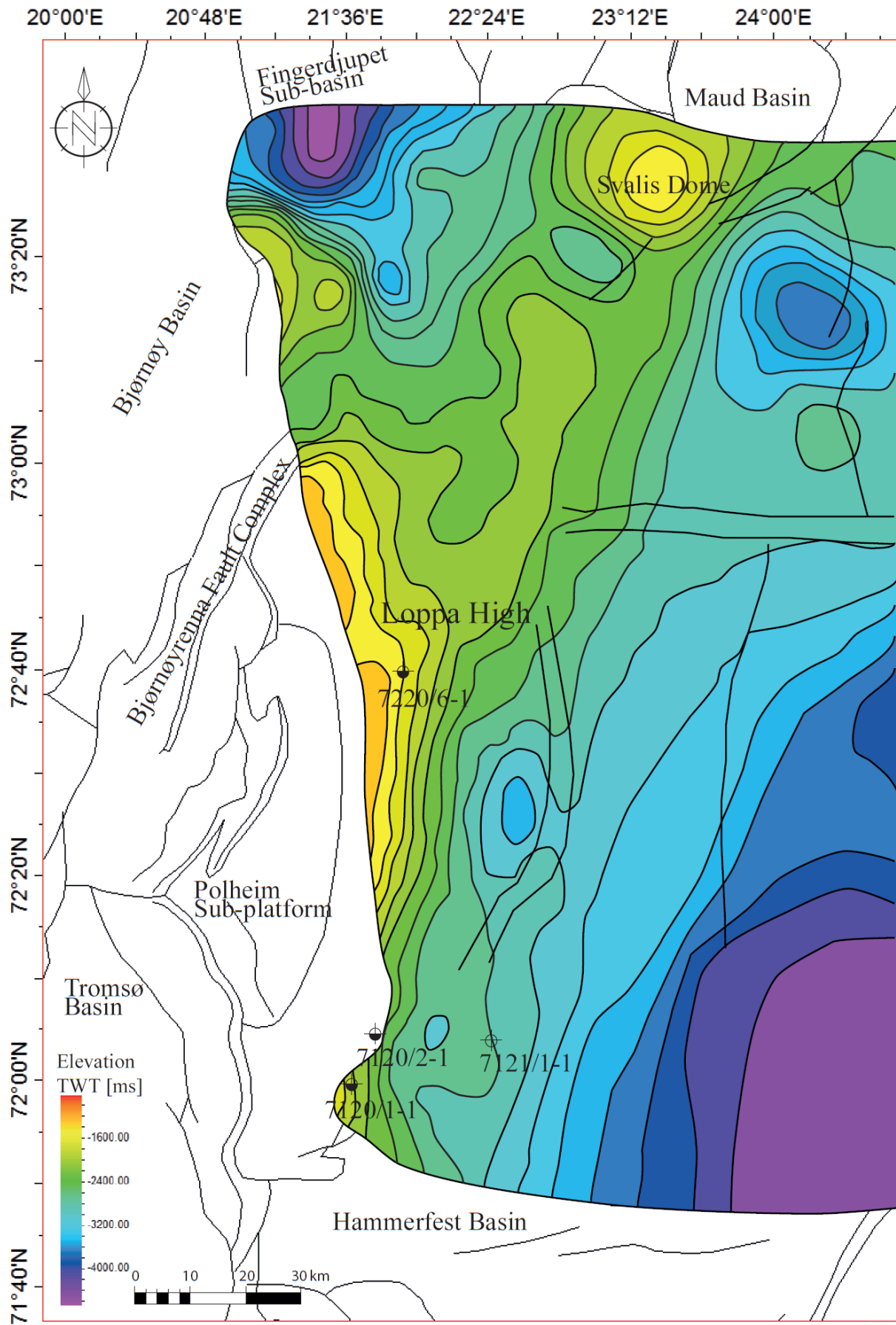


Figure 4.5 Time topographic map of the upper surface of interval 3. The surface has many similar trends to the time topographic map of top interval 1 (Figure 4.3). With a shallower western edge and a deepening towards the east and south-east. The surface is smaller than top interval 1, with exception of the east where the edge is limited by the study area. The surface is further shown as the upper boundary of interval 3 in Figure 4.8 - Figure 4.19.

4.1.4 Interval 4

Int4 has been observed only in well 7121/1-1, where the GR response is low, with some irregularity and peaking similar to Int1, while the DT. Int4 consists of the Røye Formation, which is also observed within the well section of well 7121/1-1, and marked as Int3 (Figure 4.1).

Int4 is characterized by continuous, medium to high amplitude and high frequency seismic patterns. The topographic map of the top surface of Int4, shown in Figure 4.6, has similar topographic trends as top Int1 (Figure 4.3), and top Int3 (Figure 4.5). The interval is shallowest in the western and towards the Svalis Dome and deepening to the east and south-east. Int4 is terminating by onlap to the underlying Int3 in the west, and some truncation in the shallowest areas.

In the shallowest, western part of Int4, the mounding reflectors recognised in Int3 are continuing with an aggradational stacking pattern throughout Int4. Some of the mounding reflections have a change in shape from the lowest part with circular mounding, to the top of Int4 with a more flat to a polled down top of the mounding.

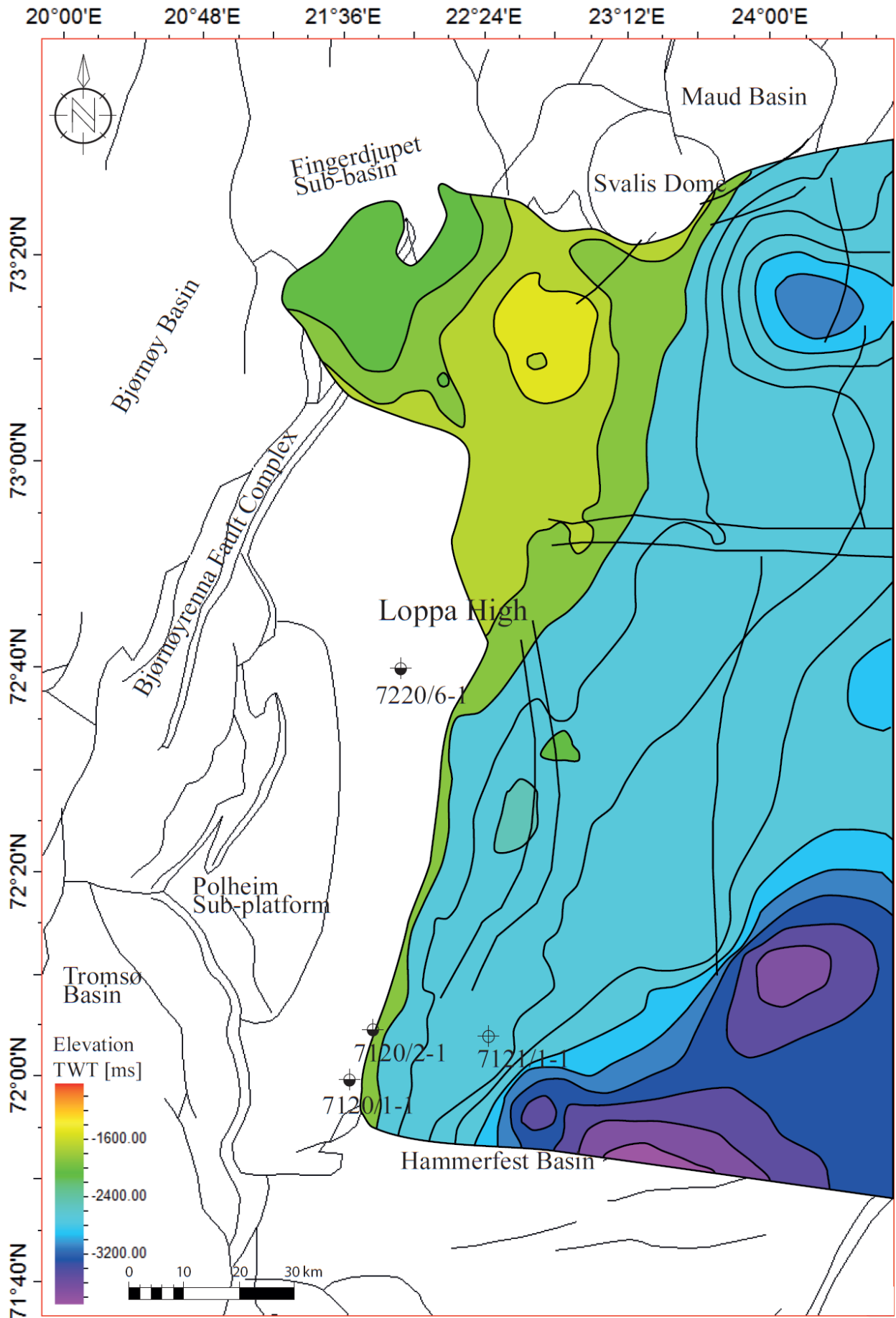


Figure 4.6 A time topographic map of the top surface of interval 4. The main trends are similar to both the top interval 1 and 2. This surface has a smaller extension, and differences in topography is smaller than for the previous surfaces. The surface is further shown as the upper boundary of interval 4 in Figure 4.8 - Figure 4.19.

4.2 Interpretation

The topographic and thickness maps shown in Figure 4.3, Figure 4.4, Figure 4.5 and Figure 4.6, coupled with the seismic sections and the geological profiles from various locations on the Loppa High as described in Figure 4.7, makes a complex geological model of the Late Palaeozoic Loppa High. This complex geological model has been used as the main utility when describing the development of Late Palaeozoic successions of Loppa High.

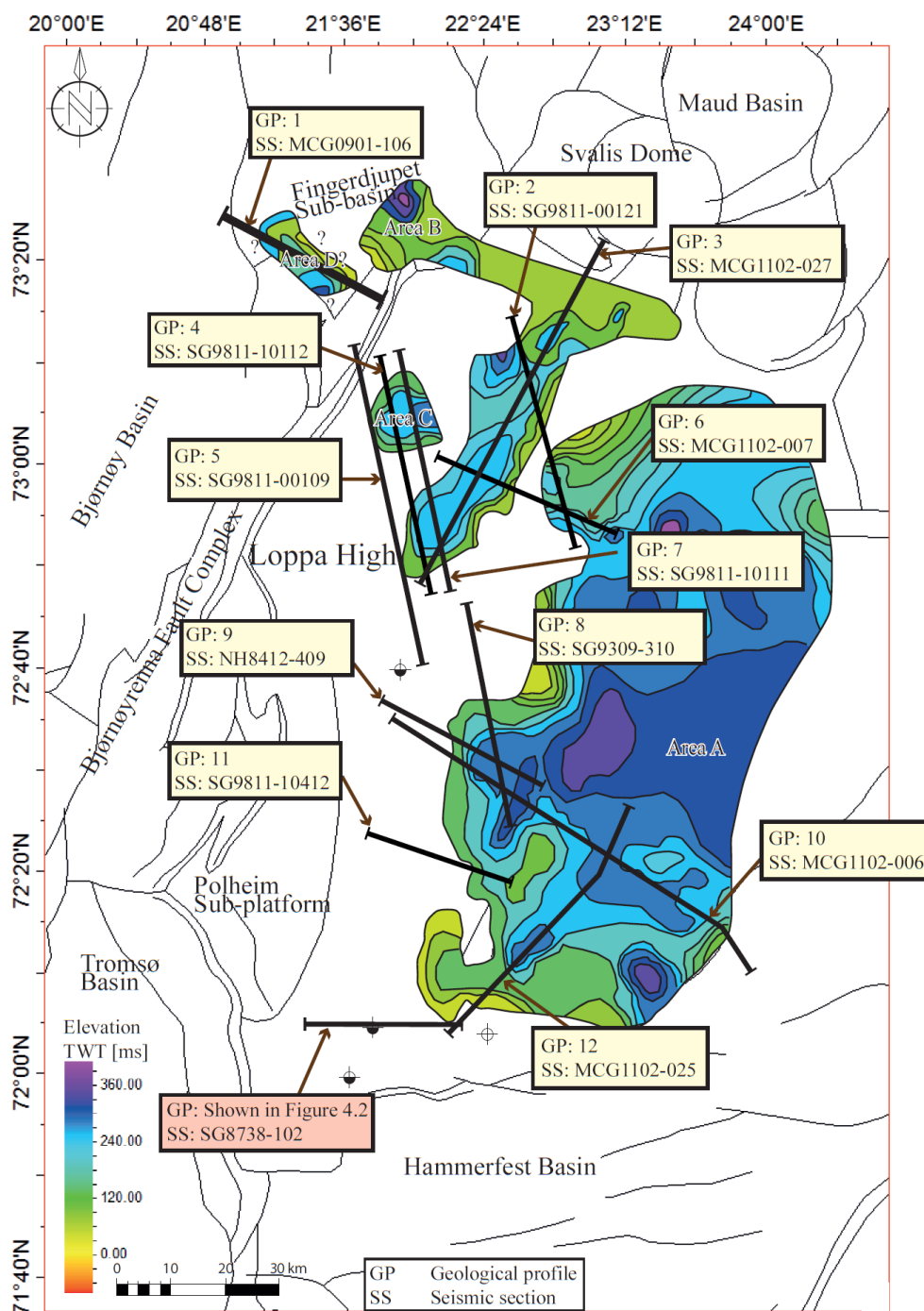


Figure 4.7 Location of geological profiles (GP) and seismic sections (SS). Black lines are showing the location of SS and GP, shown in Figure 4.8 - Figure 4.19.

4.2.1 Interval 1

Int1 is dated as a Late Carboniferous, Bashkirian – Gzhelian deposition, from the well section shown on Figure 4.1. It is a relatively thick package, probably deposited during the climatic shift from warm and humid to warm and semi-arid during Late Carboniferous time (Larsen et al. 2005). The deposition is recognised as a mix of carbonate and siliciclastic sediments, associated with the low angle paleo-structure of the Loppa High. The aggradational to progradational stacking patterns can be associated with keep-up shallow marine carbonates (as described by Kendall and Schlager (1981)) interbedded by prograding siliciclastic sediments. The truncational pattern near the western edge of the interval is probably a response to uplift phases coupled with eustatic sea level fall.

4.2.2 Interval 2

Int2 is recognised in seismic data overlying Int1 and underlying Int3, this give a maximum timespan of post Gzhelian – pre Sakmarian, as seen in the well sections in (Figure 4.1). The very high amplitude interval is recognised as evaporite, possibly deposited in sub-basins created during early uplift phases on the paleo-structure of Loppa High.

The aggrading stacking pattern and the sub-basin location of the evaporite deposits can be linked to a spill-out system which took place at a time period with lowstand sea level. The sea level may have been an isolated lowstand with carbonate production in the shallow warm water, creating ideal conditions for carbonate production. A rapid carbonate production may have created a local relative sea level rise, expanding the distribution area of the water. The larger area would then be objected to more rapid evaporation, and evaporite precipitation would be overlying the carbonates. The relatively thick package (Figure 4.4) and long depositional time span suggest multiple evaporite precipitation episodes, during seasonally low sea levels, possibly during the highly frequent and high amplitude eustatic sea level change in Late Permian, as described by Smelror (2009) and Stemmerik (1999).

The evaporite interval is sporadically distributed throughout the Loppa High. The location of Int2 depositions within the paleo sub-basins was probably separated by paleogeographic features. The location of top Int1 between area A and area B in the geological profile 2 (GP2) shown in Figure 4.9, is deeper than the base locations of the Int2 areas. This may describe a paleo-valley with deeper water level and ocean circulation, creating a high energy and non-depositional environment.

Between the norther part of area C and area B of Int2 shown in GP 4 (Figure 4.11), and also in the southern most location between area A and area B shown in GP 7 (Figure 4.14) and GP 8 (Figure 4.15), the underlying top surface of Int1 is shallower than the base location of Int2. These locations were probably shallow paleogeographic features, which may have been subaerially exposed during the lowstand episodes and resulting in non-deposition of the evaporite Int2. GP 5 is located close to the intersection area of the abrupt topographic change from the shallow south-western and the deeper valley in the north-east between area A and area B.

In GP 7 (Figure 4.14) the Int2 area C and area B is separated by a shallower paleo-geographic feature. There is also observed three high amplitude anomalies, recognised as part of Int2. The three anomalies may have separated from the main interval as a reaction of tectonic movement. Due to a shallower feature in the underlying Int1 and the older unstudied unit, which is not affected by faults, the area is believed to be shallower during the deposition of Int2. However, further post depositional uplift has probably separated the smaller anomalies from the larger areas, and might have been affected by very local salt tectonic movements, by sliding of the overlying units.

Major parts of the larger area A of Int2 is truncated, primarily in the north, east and south. The other areas of Int2 are also partly truncated and Int1 is truncated in the shallowest areas. These truncation patterns are believed to be erosional truncations and can probably be linked to the lowstand sea level and subaerially exposure during and possibly posed the evaporite deposition.

4.2.3 Interval 3

At the intersection of Int1 and Int3 in the well section of well 7120/2-1 shown in Figure 4.1, there is observed a rise in both GR and DT response. The rise is recognised as a condensed section created by a rapid rise in sea level, generating starvation and accumulation of radioactive organic matter.

Int3 is recognised as a carbonate succession deposited during the long time span of Sakmarian – Wuchiapingian. The primarily smooth and low GR and DT response gives an indication of a somewhat clean carbonate deposition, with little siliciclastic interbedding.

The carbonate succession is likely to have formed during Permian time associated with a cooler water environment (Stemmerik, 1999, Stemmerik and Worsley, 2005). Carbonate build-ups has been mapped from mounding reflections with a vertical extension from the middle until the top of Int3 Figure 4.20. The general progradational stacking pattern of Int3 gives indications of low sea level, while the aggradational build-ups can be associated with catch-up carbonates during rapid rise in sea level. The surrounding carbonate ramp may in this case have been drowned by flooding events associated with Middle – Late Permian time and resumed the carbonate production in periods with lower sea levels (Schlager, 1989, Sayago et al., 2012).

4.2.4 Interval 4

From the well section (of well 7120/1-1 in Figure 4.1) Int4 is recognised as a Late Permian, Changhsingian succession consuming the Røye Formation. Well 7120/1-1 is also penetrating the Røye Formation, which in this section is both overlying and underlying the Ørret Formation. This part of Røye Formation can probably be related to Int4, but the seismic trace of Int4 cannot be found at the shallower well location. However, there might be a thin succession that is not visible on seismic data, or the succession might be eroded and is therefore missing from the majority of the shallower areas.

Ørret Formation (part of Int3) generally consumes shallower siliciclastic sediments, while the Røye formation is recognised as a somewhat deeper carbonate succession. This formation intersection can therefore be a direct link to a change in sea level position. The lowermost Ørret Formation is probably deposited at the well location during a lowstand, followed by a rise in sea level allowing the middle shelf carbonates of the Røye Formation to back-step towards the shelf overlying Ørret Formation. This is followed by a repeated lowstand and deposition of siliciclastic sediments overlying the carbonates succession.

The aggradational carbonate build-ups recognized in Int3 are observed to extend into the shallowest parts of Int4, as shown in GP 2 (Figure 4.9), GP 3 (Figure 4.10), and GP 5 (Figure 4.12). The uppermost build-up is vertically extending above the reminding carbonate ramp of Int4. The shallower carbonate build-ups can indicate a catch-up carbonate system, surrounded by an occasionally drowned carbonate ramp.

There is also observed three build-up features with a somewhat ring-shaped upper rim and a semi-circular depression, creating an atoll like shape (shown in Figure 4.12 and locations of the atoll features in Figure 4.20). An atoll is a coral reef that encloses a lagoon partly or completely, and is therefore a clear link to a sea level lowstand (Schlager and Purkis, 2013). The atolls are located on the western margin of Int4, slightly deeper than the main trend of the carbonate build-ups. This is probably due to a generally lower sea level during the development of Int4, then during the build-up development, generally consumed in Int3.

The overlying Triassic sediments onlapping Int4 and are recognised as almost horizontal reflections on the seismic data. The major tectonic uplift events probably cease during Late Permian – Early Triassic, leaving the pre deposits in approximately location of deposition (Sayago, 2014).

GPI

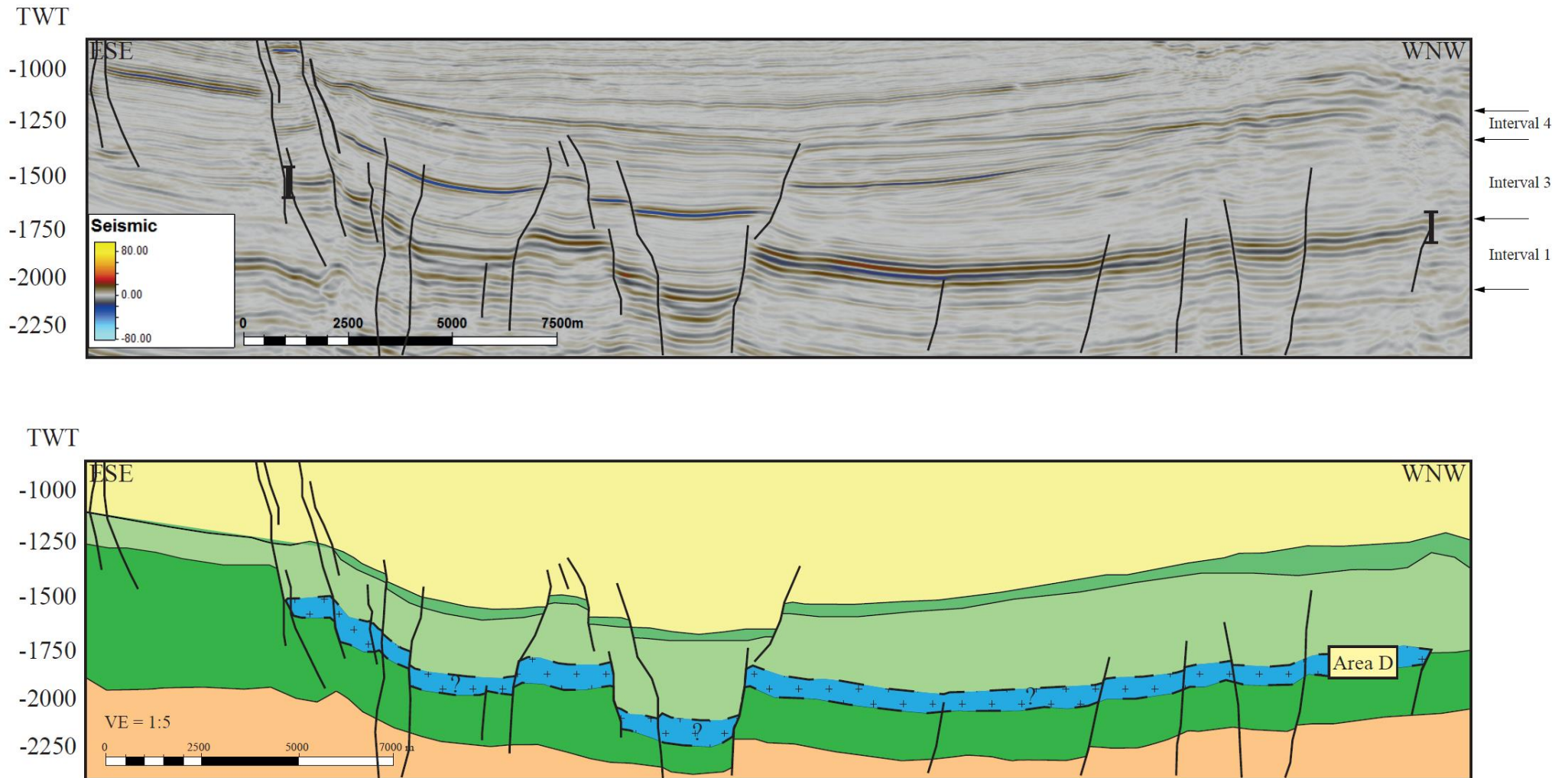


Figure 4.8 Geological profile 1. The 2D line MCG0901-00121 (top illustration) is mapped with the interval top and base shown on the right side, and terminations of interval 2 shown with black lines. The interpreted geological profile (base illustration) shows the distribution of the four main intervals within the section. Area D of interval 2 is marked by question marks due to high uncertainty of the area. Location is shown on Figure 4.7, and legend is shown on Figure 4.2

GP2

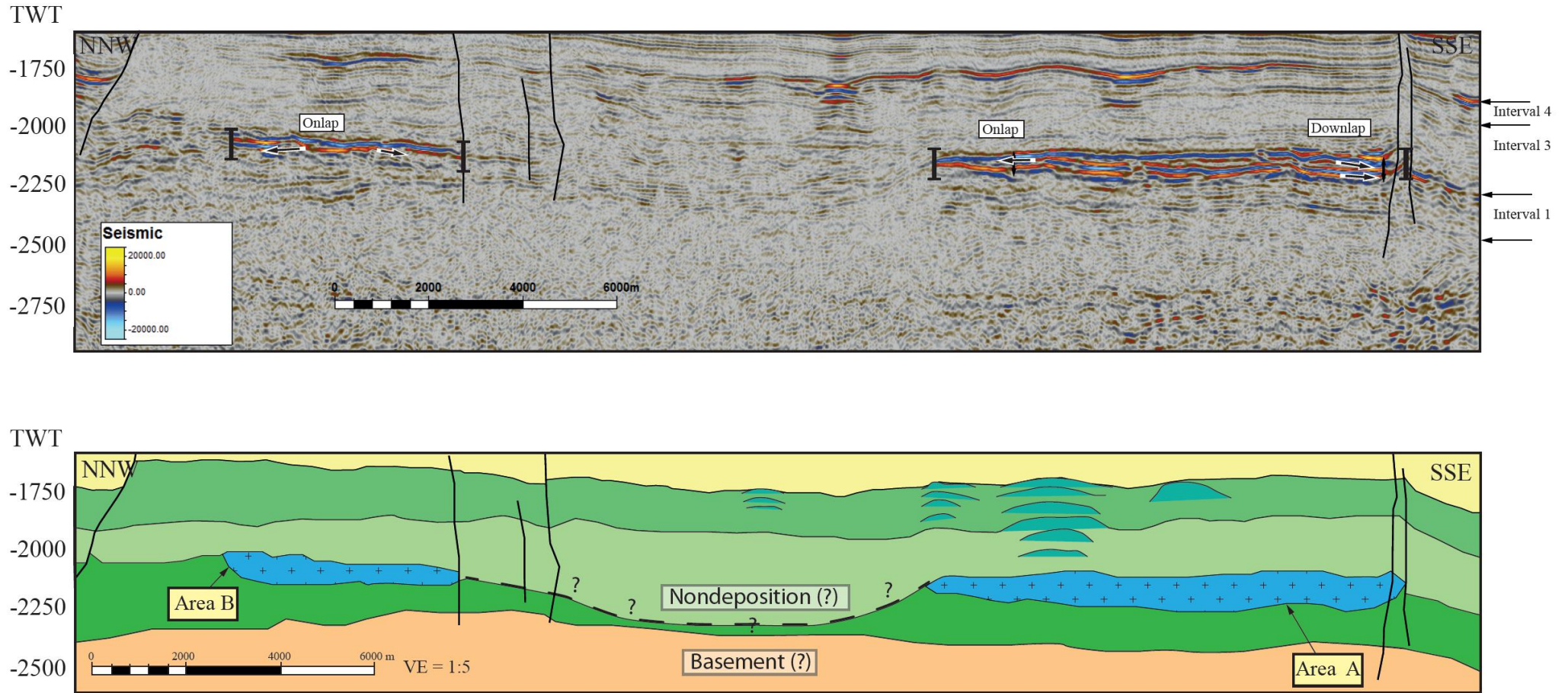


Figure 4.9 Geological profile 2. The seismic section SG9811-00121 has been mapped with the deepest part of top surface interval 1 between the two areas of interval 2. Interval 2 contains onlap and downlap patterns, terminating on the top surface of interval 1. Aggradational mounding reflections are building up from the middle of interval 3 until the top of interval 4. Location is shown on Figure 4.7 and legend is shown on Figure 4.2.

GP3

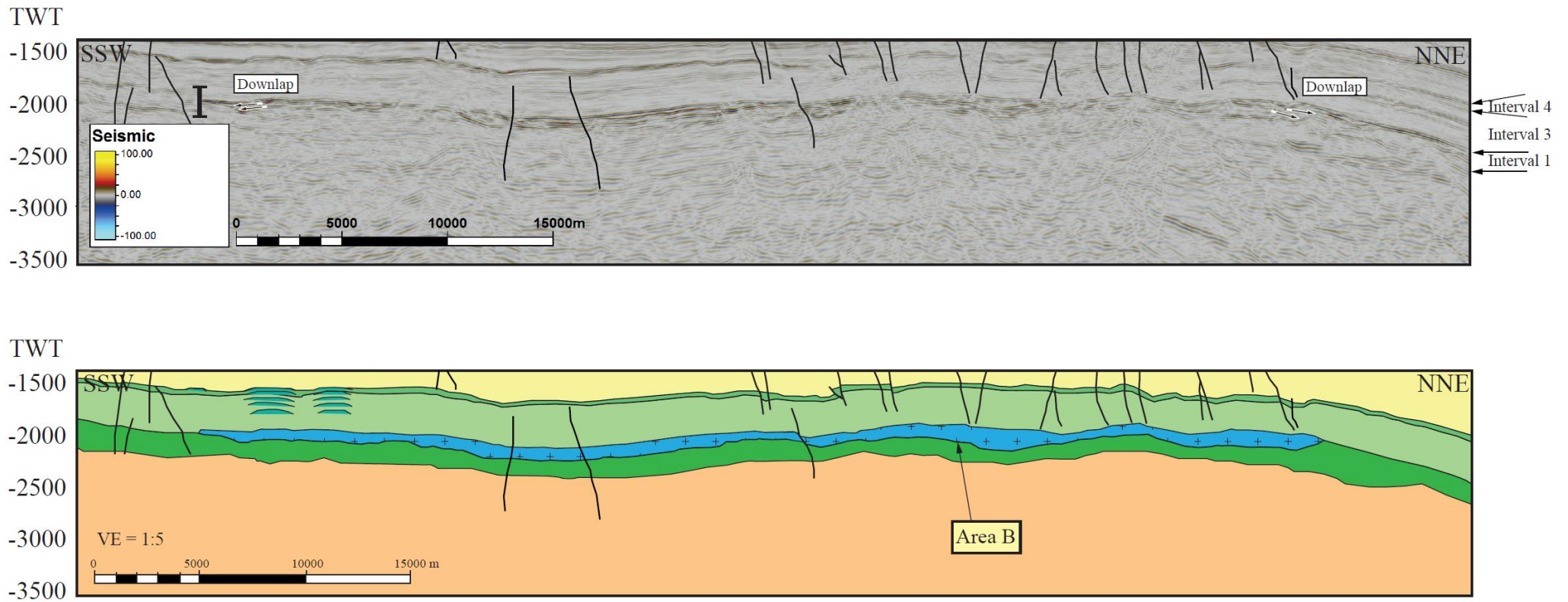


Figure 4.10 Geological profile 3. The seismic section MCG1102-027 is located on the northern Loppa High. Interval 1 is in parts difficult to distinguish from the underlying unit. Interval 2 terminates the underlying surface by downlap. Aggradational mounding reflections are present in the south south-west, from the middle of interval 3 until the top of interval 4. Location is shown on Figure 4.7 and legend is shown on Figure 4.2.

GP4

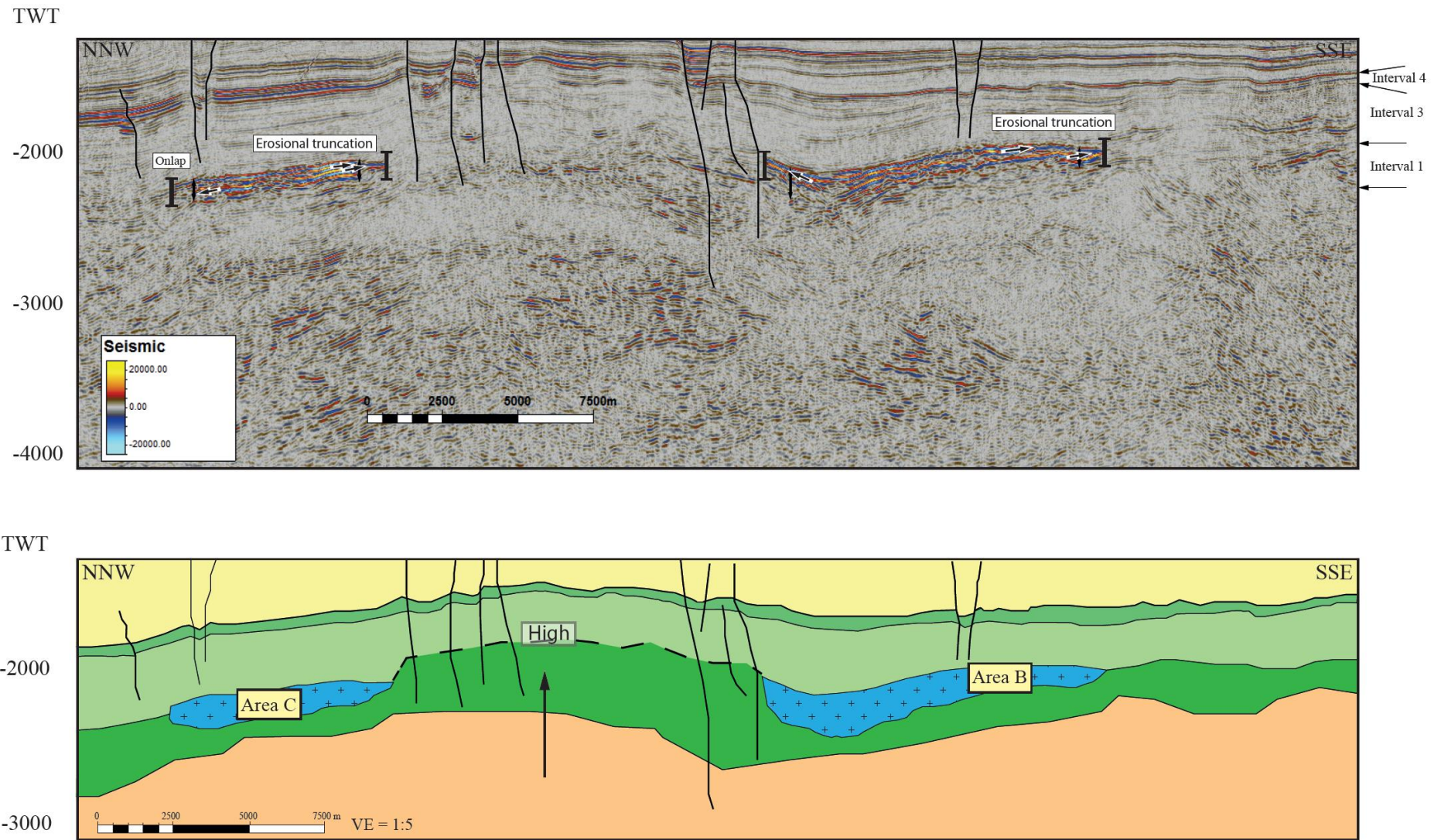


Figure 4.11 Geological model 4. The seismic section SG9811-10112 is located on the north-western Loppa High. Interval 1 is shallowest between the two areas of interval 2. Interval 2 contain truncation patterns in the south south-east margins. Location is shown on Figure 4.7, and legend is shown on Figure 4.2.

GP5

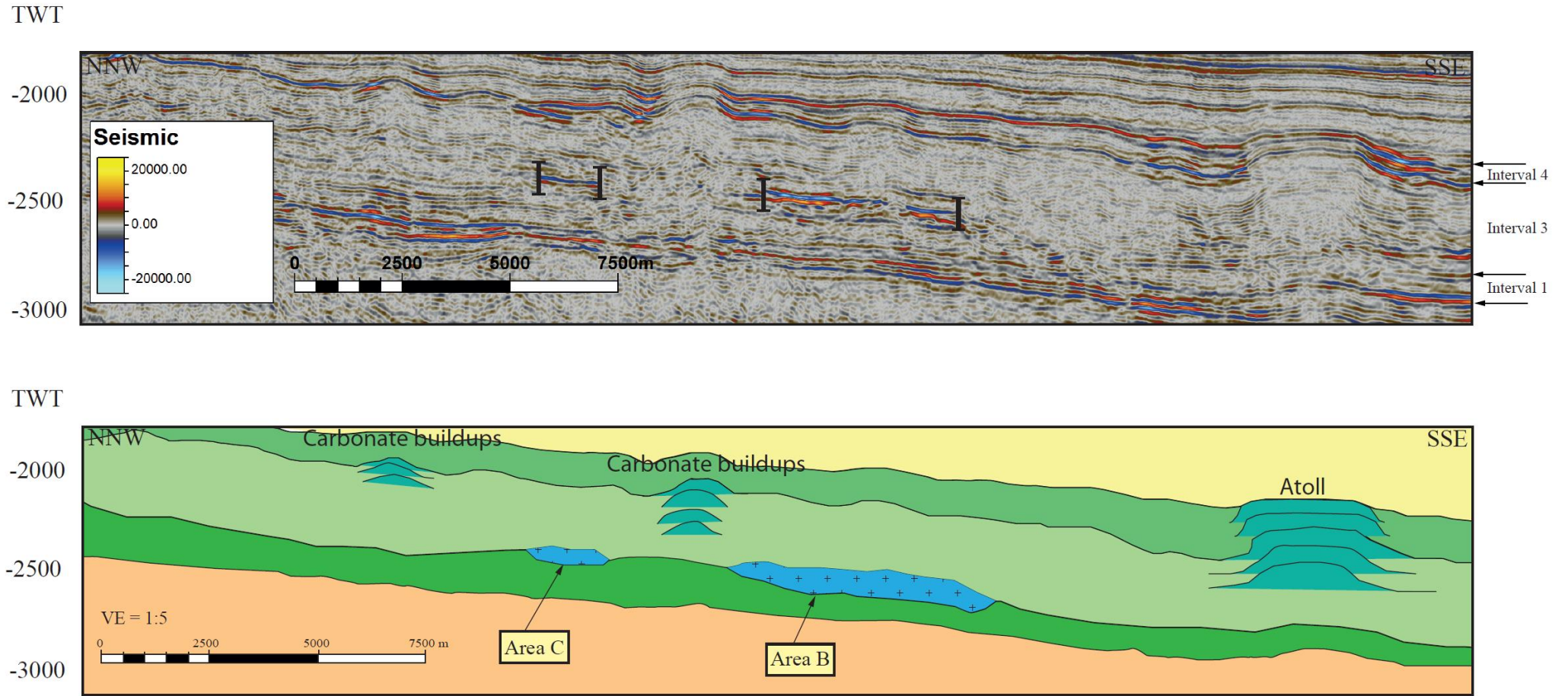


Figure 4.12 Geological profile 5. The seismic section SG9811-00109 shows the southern edges of both area C and area B of interval 2. The top surface of interval 1 is slightly shallower between area C and area B, then in the location underlying interval 2. Aggradational mounding reflections are present from the middle of interval 3 until the top of interval 4. The central and north north-west mounding reflections are recognised as carbonate build-ups, and the south south-west mounding reflections are recognised at the base as a carbonate build-up and at the top as a carbonate atoll due to a circular rim geometry. Location is shown on Figure 4.7, and legend is shown on Figure 4.2.

GP6

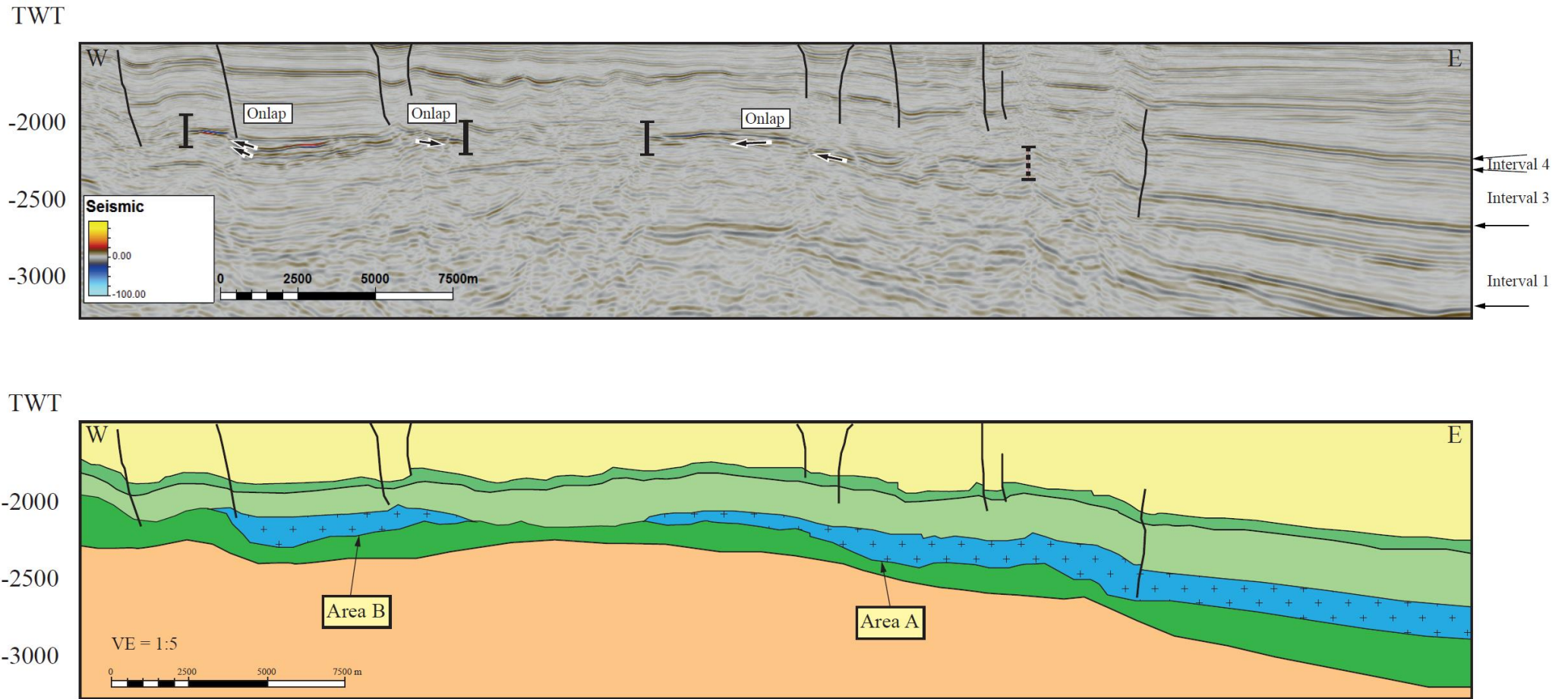


Figure 4.13 Geological profile 6. The seismic section MCG1102-007 is located in northern part of Loppa High and highly affected by faults. Interval 2 terminates by onlap, and continues from area A and east with more continues reflections. Location is shown on Figure 4.7, and legend is shown on Figure 4.2.

GP7

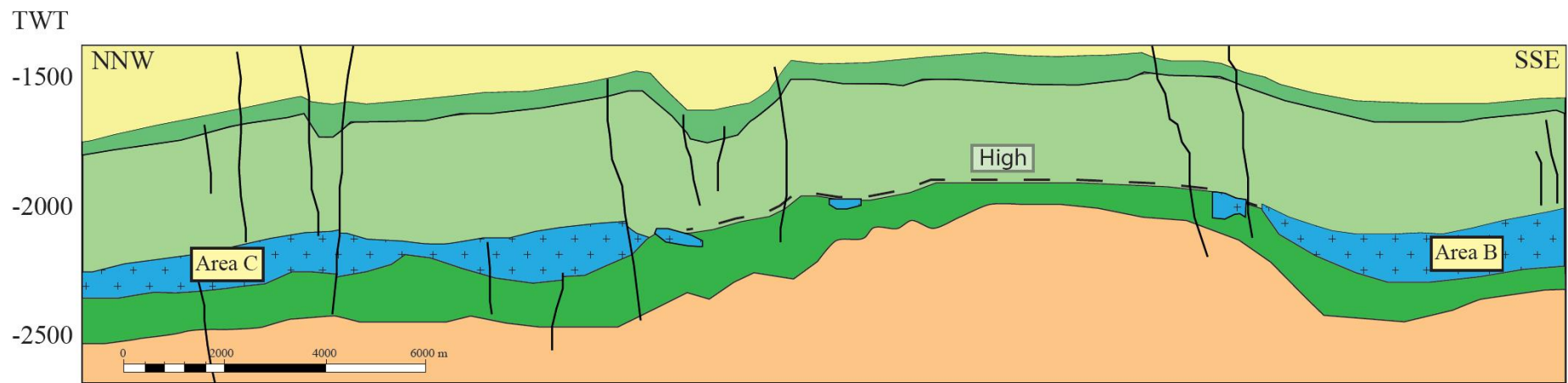
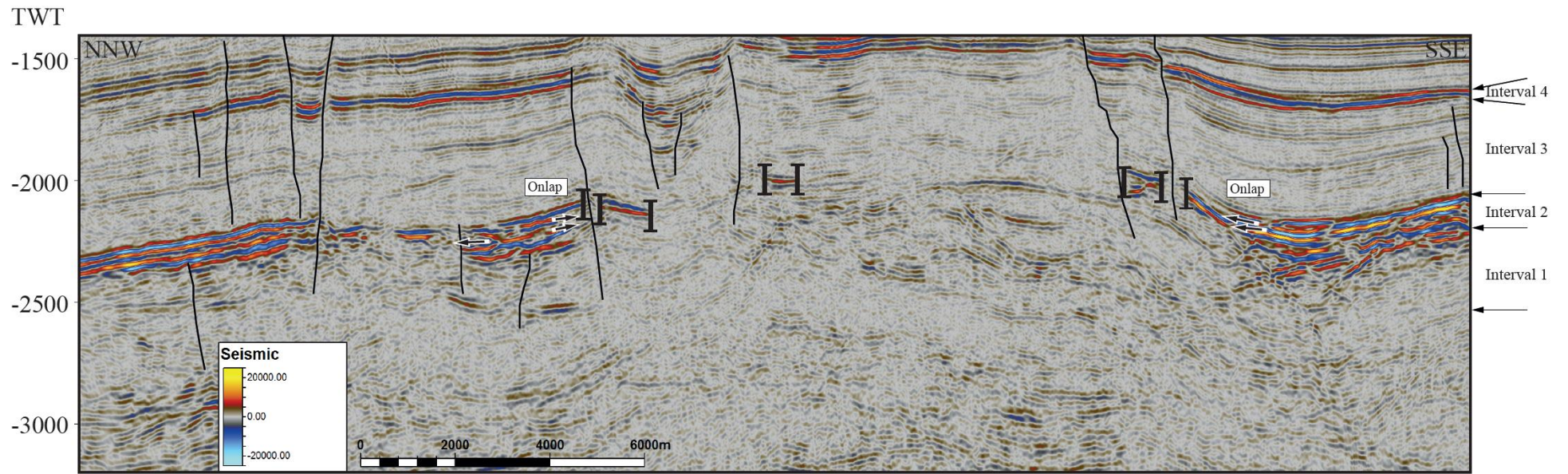


Figure 4.14 Geological profile 7. The seismic section SG9811-10111 is located in the north-west Loppa High. The main intervals are shallowest in the location between area C and area B of interval 2. Location is shown on Figure 4.7, and legend is shown on Figure 4.2.

GP8

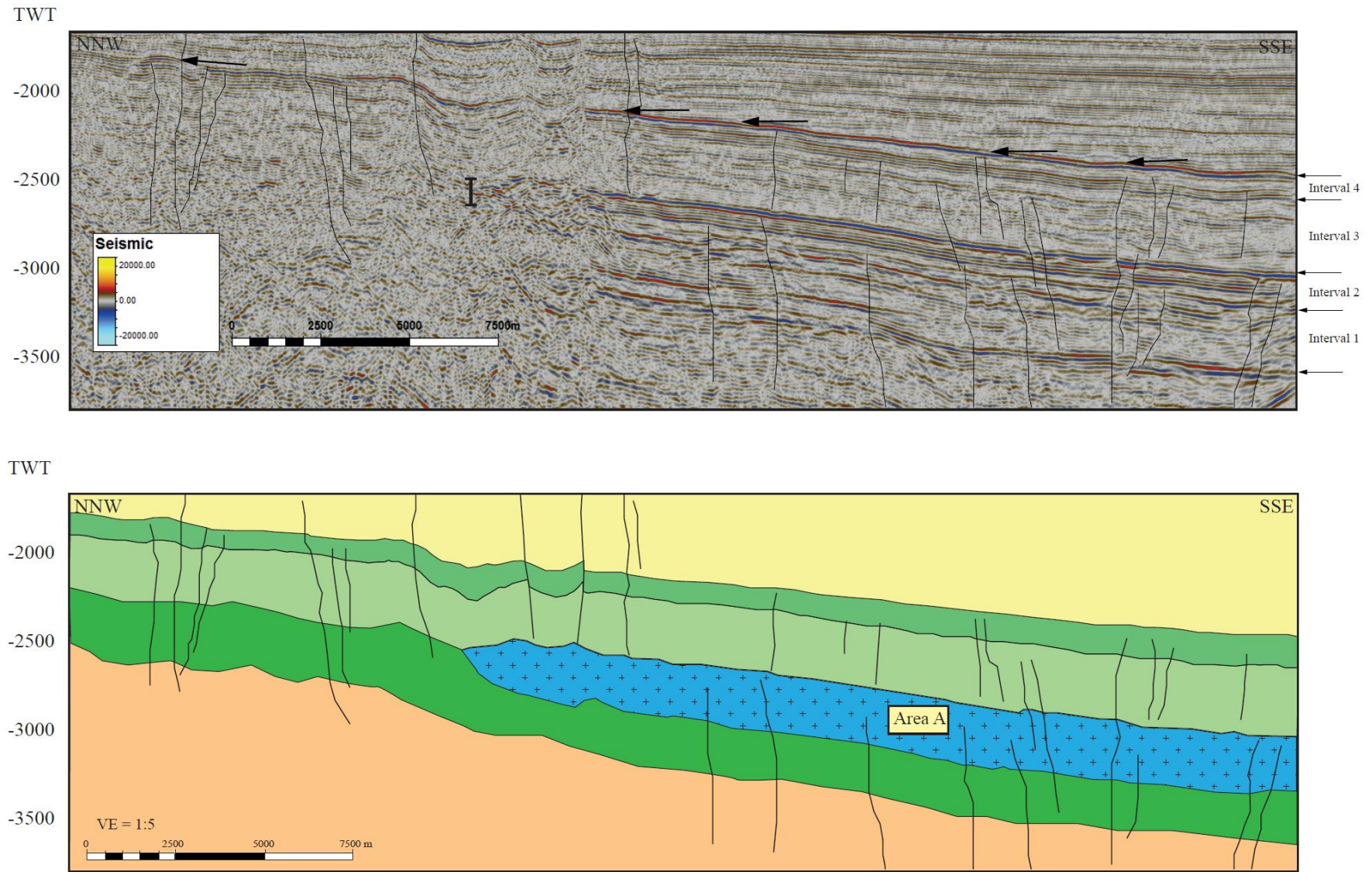


Figure 4.15 Geological profile 8. The seismic section SG9309-310 is located in the central Loppa High and is shallowest in the north north-west. The termination of interval 2 is recognised as onlap, but is disturbed by faults and possible gas migration. Location is shown on Figure 4.7, and legend is shown on Figure 4.2.

GP9

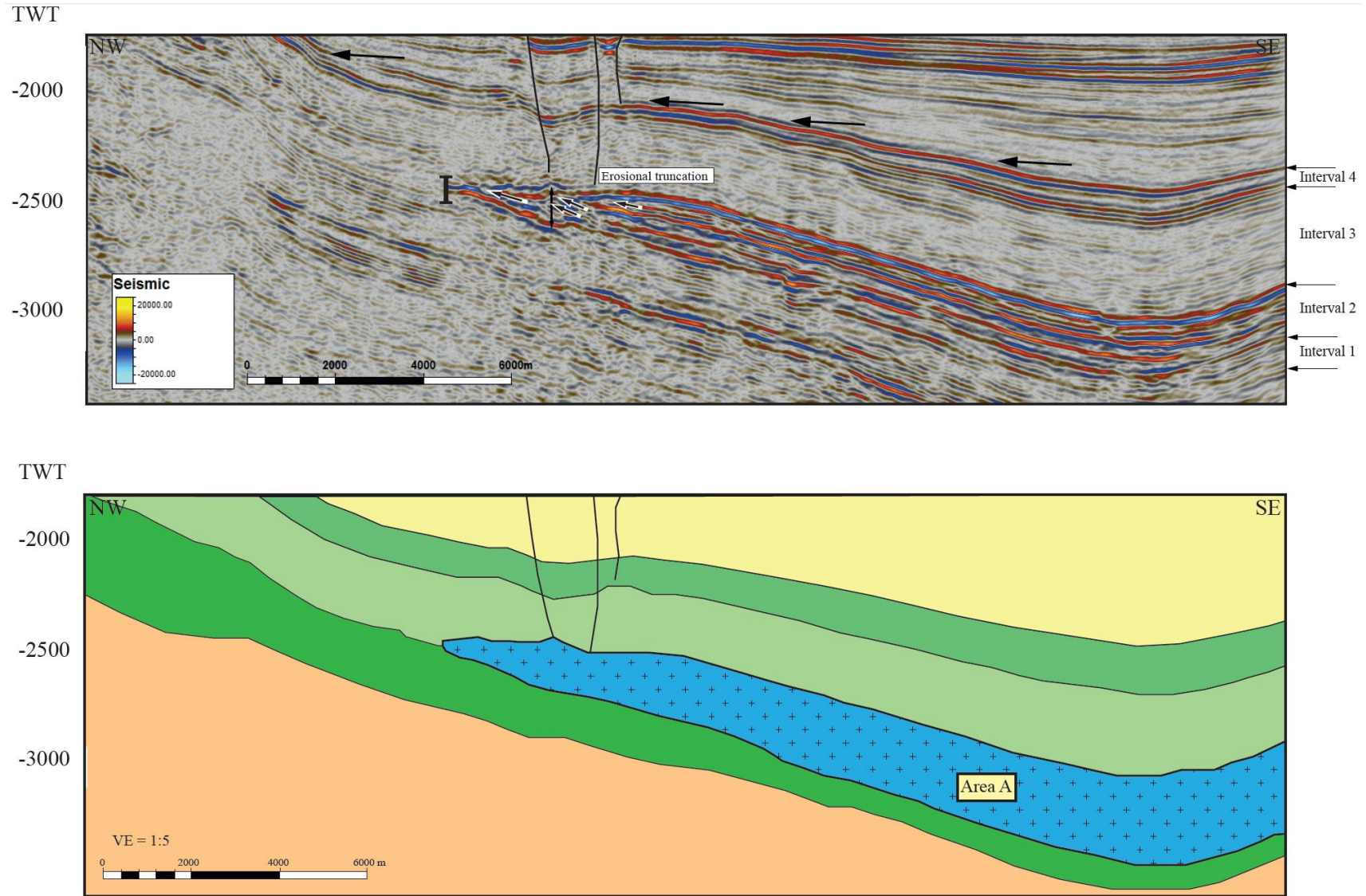


Figure 4.16 Geological profile 9. Seismic section NH8412-409 the main interval is shallower in the north-west and deepening to the south-east. Interval 2 is truncated in the shallower north-west. The Triassic unit overlying interval 4 is in the section clearly onlapping the top surface of interval 4. Location is shown on Figure 4.7, and legend is shown on Figure 4.2.

GP10

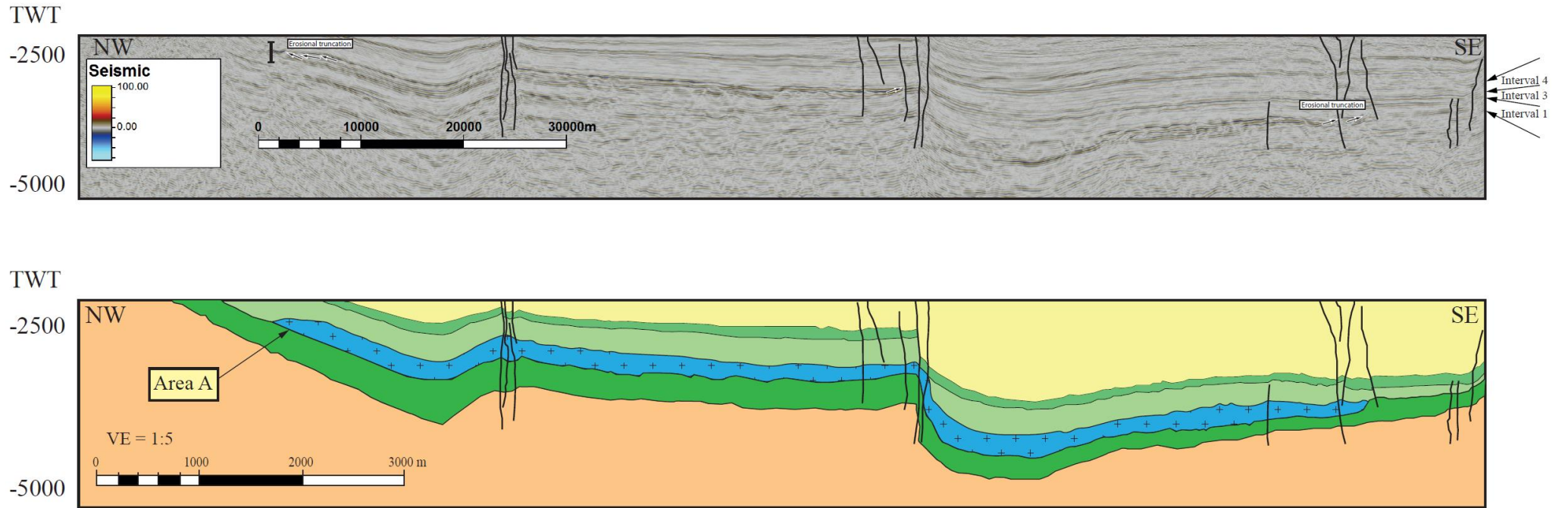


Figure 4.17 Geological profile 10. Seismic section MCG1102-006 is shallowest in the north-west near Loppa High, and is deepening to the south-east Hammerfest Basin. Interval 2 is recognised to terminate by truncation in both the north-west and south-east. Location is shown on Figure 4.7, and legend is shown on Figure 4.2.

GP11

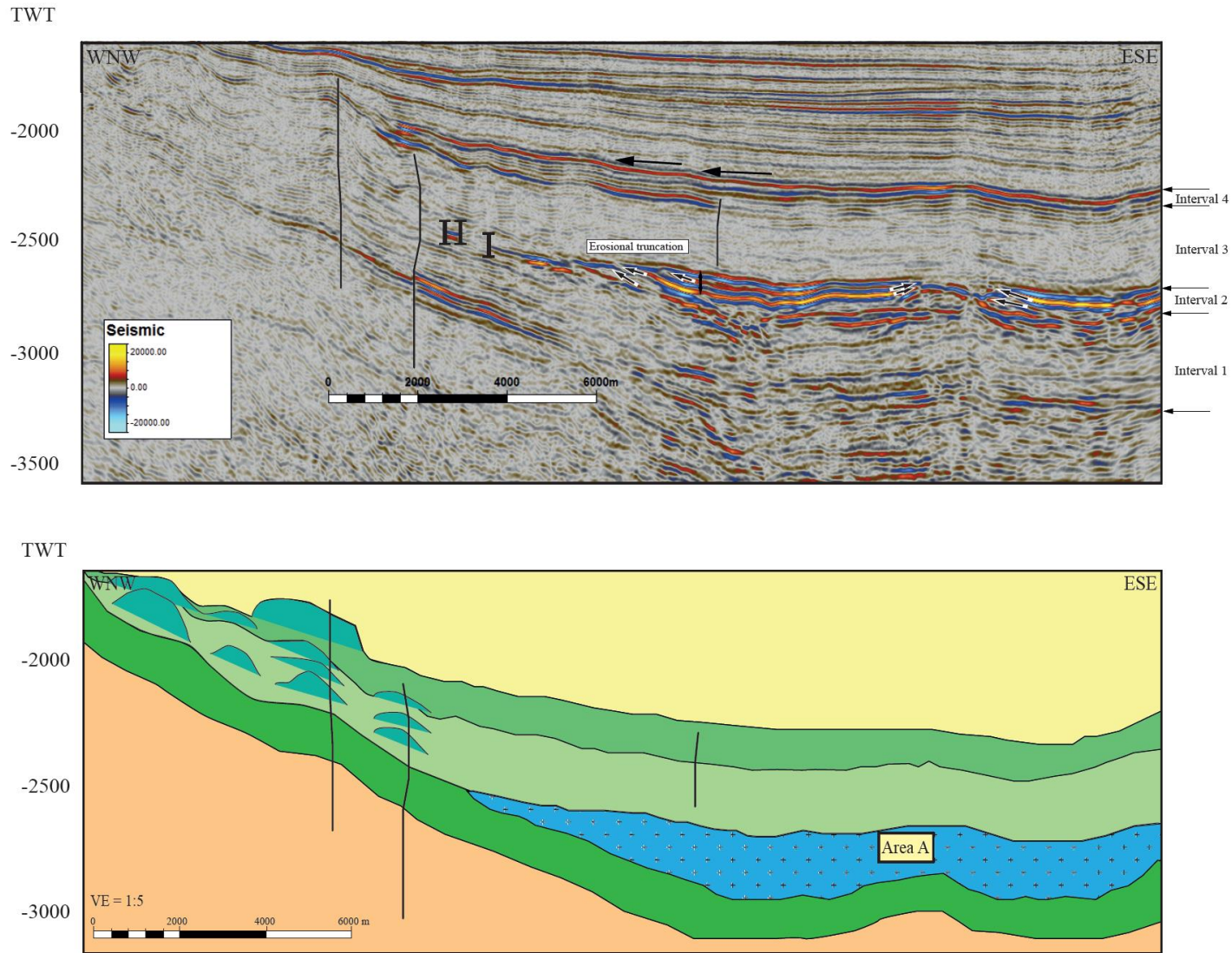


Figure 4.18 Geological profile 11. Seismic section SG9811-10412 shows interval 2 in the deepest east south-east part, with truncation patterns towards the shallower west north-west. Location is shown on Figure 4.7, and legend is shown on Figure 4.2

GP12

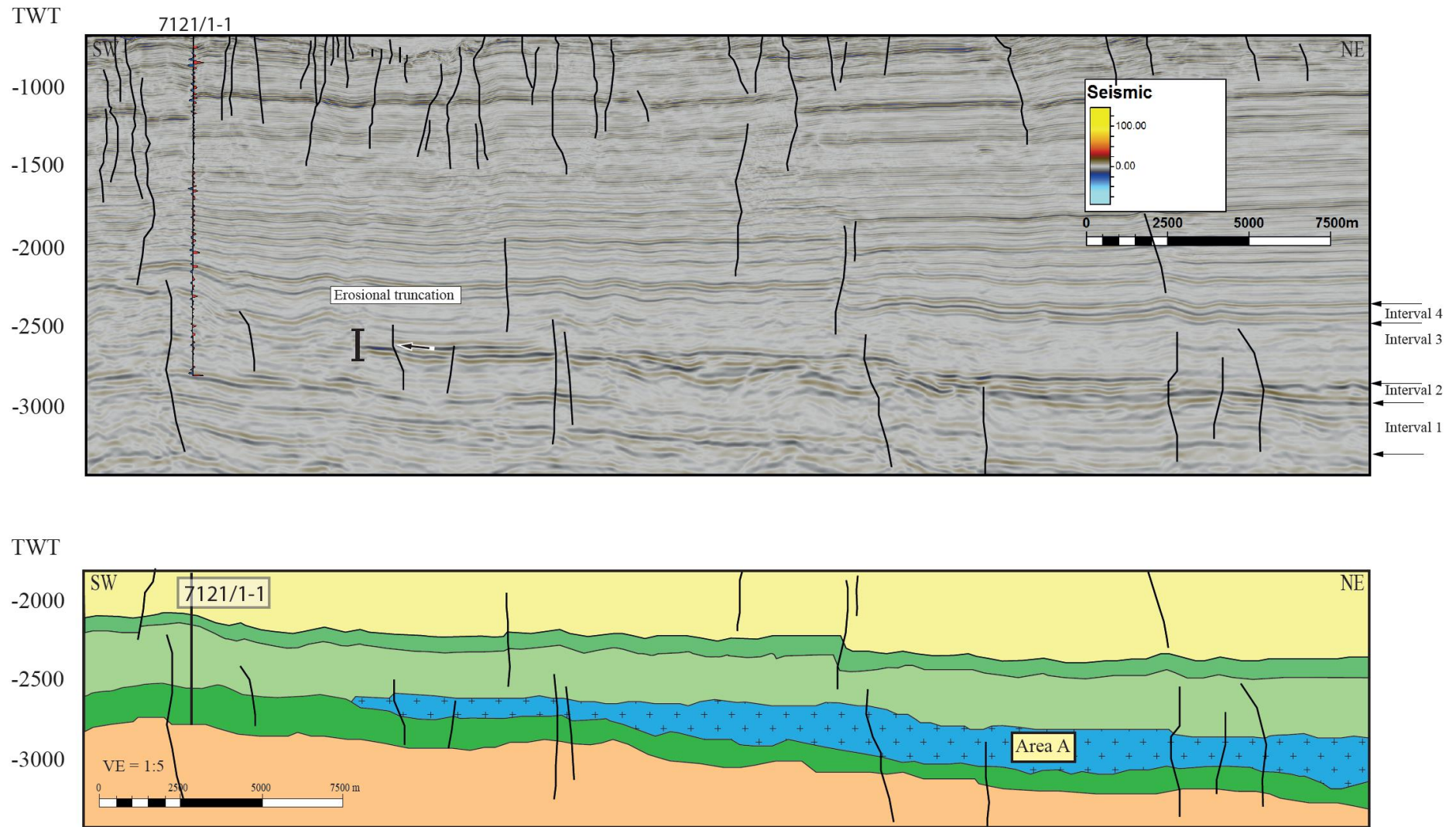


Figure 4.19 Geological profile 12. Seismic section MCG1102-025 is located in the southern Loppa High. Well 7121/1-1 has been used to correlate interval 1, 3 and 4. Interval 2 is truncated in the shallower south-west. Location is shown on Figure 4.7, and legend is shown on Figure 4.2.

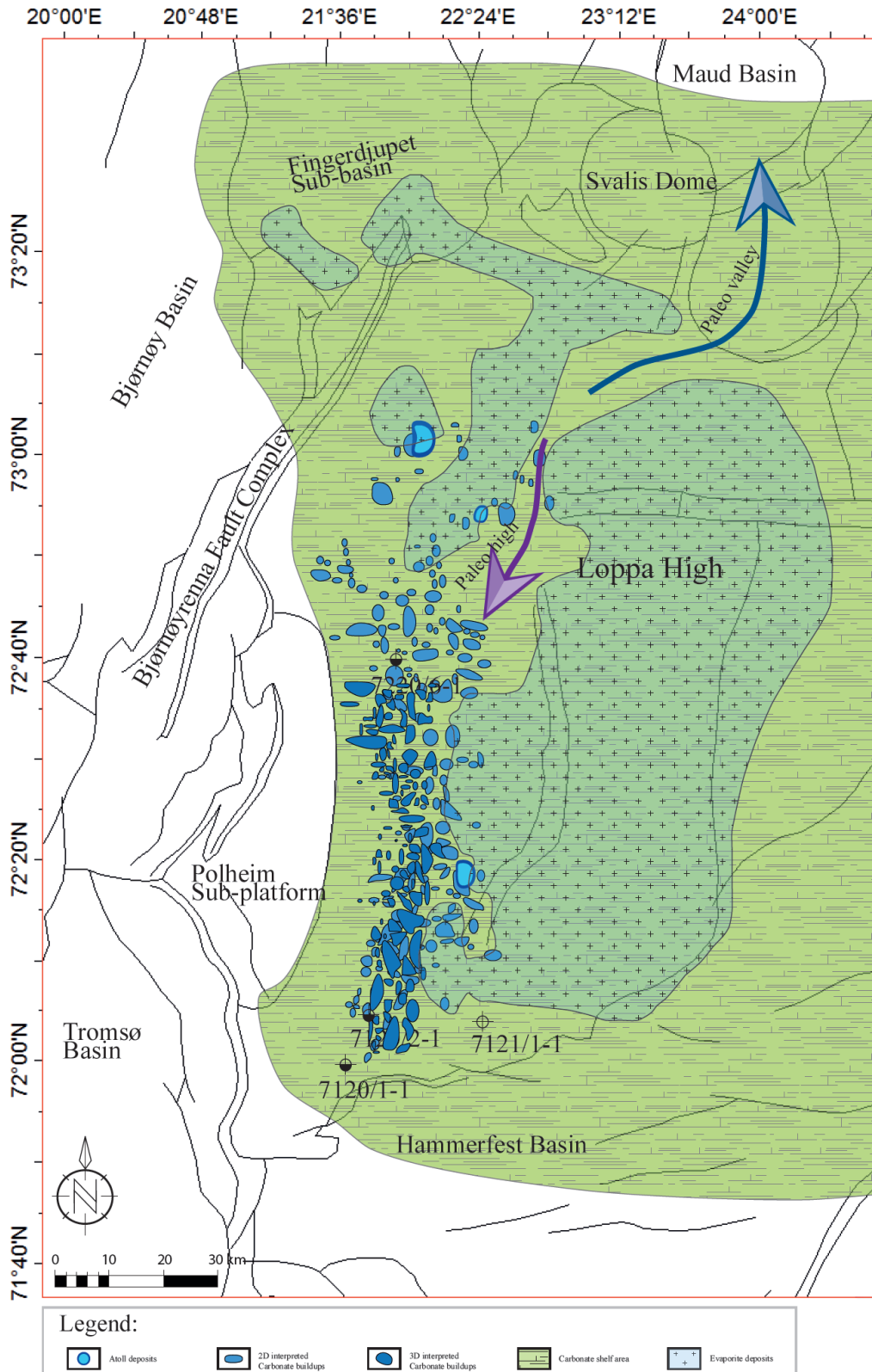


Figure 4.20 Facies map of Late Palaeozoic successions on Loppa High. The carbonate ramp is displayed (green) with the underlying interval 2 recognised as evaporite (blue body) and mounding reflections from interval 3 and interval 4 as carbonate build-ups (blue circles). The blue arrow is illustrating a paleo-valley and the purple arrow is illustrating a shallower paleo-high. The majority of the build-ups are observed only in few 2D lines, resulting in uncertainty of the build-ups geometry.

5. Discussion

The Late Palaeozoic climate on the Loppa High was affected by the northward drift post to the brake-up of the supercontinent Pangea (Stemmerik, 1999, Stemmerik and Worsley, 2000, Stemmerik and Worsley, 2005). Local tectonic movements are believed to have formed a specific depositional environment restricted to the Loppa High with ideal conditions for carbonate production.

Loppa High has been objected to climatic change, sea level change, and uplift previous to and during the development of Late Palaeozoic successions. The Loppa High is regarded as a tilted ramp, with a depositional slope of less than 5° by the onset of Late Palaeozoic time. The tilted ramp creating differences in local depositional environments and agrees with Sarg (1988) definition of a regional carbonate ramp. The largest uplift phase the Loppa High has been affected by is recorded to occur during the end of Late Palaeozoic to Early Triassic time (Larssen et al., 2005).

The three intervals recognised in the well sections seen in Figure 4.1, all show low GR and DT responses. The intervals have consequently been recognised as carbonate successions and correspond to the well log response of carbonate described by Asquith and Gibson (1982). While Int2 has been recognised as an evaporite deposition interbedded by carbonates, due to the high amplitude and uncontinues reflectors, as well as comparisons with research done in nearby areas (Larssen et al., 2005, Sayago, 2014).

5.1 Paleogeography and sea level change on Late Palaeozoic Loppa High

The topographic maps of top Int1 (Figure 4.3), Int3 (Figure 4.5) and Int4 (Figure 4.6) are based on seismic data as it can be observed today and are not replica maps of the paleogeography of the Late Palaeozoic Loppa High. The paleogeography is believed to have evolved in multiple phases during Late Palaeozoic time. The gradual uplift and tilting coupled with sea level change has been the main control of the paleo-landscape and the depositional environment.

5.1.1 Carboniferous

The depositional onset of Int1 is associated with the Visean warm tropical climate, ideal for carbonate production (Stemmerik, 1999). Tectonic movement was the main control on the depositional environment during Visean – Sarpukhovian. The tectonic movement was combined with a regional transgression, which increased sedimentation with aggradational carbonate production mixed with progradational siliciclastic sediments (Stemmerik, 1999, Stemmerik and Worsley, 1989). The following rifting phases gradually ceased during Late Bashkirian time, and the depositional environment was controlled by a regional rise in sea level, creating an eastward thickening of Int1 (Stemmerik and Worsley, 1989).

The climate during Serpukhovian – Bashkirian changed from warm and humid to warm and arid. There has also been recorded a gradual shift on the western Loppa High depositions from continental to marine, during the time span from Bashkirian – Early Moscovian (Larssen et al., 2002, Larssen et al., 2005, Stemmerik and Worsley, 1989).

Tectonic activity on Loppa High decreased in Late Bashkirian – Late Asselian (Stemmerik, 1999, Stemmerik and Worsley, 1989). A general rise in sea level is described during the same time period by the sea level curve of Haq and Schutter (2008). The rise in sea level is believed to have flooded the entire Barents Sea and the period was characterized by carbonate platforms separated by deep water basins (Stemmerik and Worsley, 2000). The world was at this time affected by icehouse conditions, creating frequent sea level change (Soreghan and Giles, 1999, Wright, 1992).

It can be suggested that the start of the evaporite precipitation of Int2 was deposited in sub-basins already during the warm semi-arid to arid Kasimovian time, accompanied with tectonic movements and further tilting of the Loppa High ramp (Sayago, 2014, Stemmerik and Worsley, 2000). Frequent and high amplitude sea level changes have been described in this time period. During Kasimovian there was at least three sea level lowstands, as described on the sea level curve of Haq and Schutter (2008).

5.1.2 Permian

Due to early uplift phases and eustatic sea level drop by the onset of Early Permian, it is possible that the Loppa High was exposed, terminating the carbonate production and eroding the pre deposited carbonate Int1 (Sayago, 2014).

Early Permian was in the western Barents Sea affected by a warm and arid to semi-arid climate and tectonic uplift phases. However, the Asselian is generally an age associated with

icehouse conditions on the southern hemisphere (Smelror et al., 2009). The sea level was at this time period highly affected by the glacio eustatic change and a series of seasonally lowstands (Haq and Schutter, 2008, Nielsen et al., 2013). The tectonic uplift coupled with the lowstand sea level probably led to an isolated ocean in the Loppa High region. The isolated oceans combined with the warm climate and the local sub-basin structures on the Loppa High are believed to have formed a spill-over system, as described by Kendall et al. (1991). The warm and shallow water led to rapid carbonate production and local sea level rise due to the carbonate accumulation. The local waters of the sub-basins were therefore extended to a larger area and increased evaporation, resulting in evaporite precipitation. The spill-over system is believed to have taken place in multiple phases during the seasonal eustatic lowstands, creating a thick package of aggradational evaporite deposits.

A shift to a cooler climate accompanied with a flooding event on the central Pangean northern margin has been recorded in Early Sakmarian time (Stemmerik, 1999, Stemmerik and Worsley, 2005). This event is associated with major melting phases on the southern hemisphere, and marks the end of the seasonal eustatic change in sea level and probably the evaporite precipitation of Int2 (Stemmerik and Worsley, 2000, Stemmerik and Worsley, 2005). The onlap to downlap patterns of Int3 suggest a rapid rise in sea level and the extensive build-ups from the middle to upper Int3 are likely to have started developing during the Early Sakmarian flooding (Stemmerik, 1997, Stemmerik, 2008).

Extensive uplift of structural highs on the central northern margin of the Pangean shelf took place in Late Sakmarian – Artinskian (Nilsson, 2001, Stemmerik and Worsley, 2005). This uplift phase affected the Loppa High and resulted in erosional truncation of Late Palaeozoic carbonate successions by the western margin of the Loppa High (Stemmerik, 1999, Elvebakk et al., 2002).

A gradual deepening has further been linked to a Kungurian hiatus and the drowning of carbonate successions, followed by a long period of non-deposition (Schlager, 1989). The carbonate build-ups are believed to have developed as catch-up systems extending towards the sea surface during the rise in sea level and drowning of the surrounding carbonate shelf (Alves, 2016, Schlager, 1981).

Build-ups recognised in Int4 are extending features of the build-ups seen in Int3. Due to the circular rim shapes seen in the upper part of some build-ups of Int4, the relative sea level on the Loppa High is believed to have a lowstand episode by the end of Late Permian time. The

circular rim is seen as a consequence of waves and tidal water and is therefore recognised as a shallow water feature. The retrogradational stacking pattern recognised in Int4 may reflect a rapid subsidence in the eastern Loppa High and surrounding basin. While the more aggradational trend in the shallower western Loppa High may suggest a keep-up carbonate system affected by minor subsidence (Bosence, 2005, Bosence et al., 1998, Brachert and Stueckrad, 2002, Cross et al., 1998, Purser et al., 1998, Purser and Bosence, 2012, Ruiz-Ortiz et al., 2004).

The carbonate build-ups recognised in Int3 and Int4 are expected to evolve in a vertical direction towards the sea surface. The eastward tilting trend seen in the seismic data is therefore a good indication of tectonic activity post to the build-up development.

Carbonate production at the end of Late Permian is linked to a major uplift phase on the Loppa High, creating further tilting and subsidence in the east (Larssen et al., 2005, Gudlaugsson et al., 1998a). The uplift phase was accompanied by a cooler climate and change in ocean circulation, distributing high energy cold water in the region (Beauchamp, 1994, Beauchamp and Baud, 2002, Ehrenberg et al., 1998, Larssen et al., 2005). The event is recognised with a shift from carbonates to siliciclastic depositions (Sayago, 2014).

The shift from Late Permian carbonate to the overlying Triassic sediments has been discussed as a possible unconformity and a drowned carbonate shelf. However, due to limited data, researchers have not been able to exclude the possibility of a subaerial exposure and a major hiatus between the Late Permian carbonates and the Triassic siliciclastic sediments (Beauchamp, 1994, Beauchamp and Baud, 2002, Ehrenberg et al., 1998). The major uplift phases of the Loppa High generally ceased out after the major Late Permian event, leaving the post deposited Triassic successions at a position approximately similar to where they can be seen on seismic sections today (Sayago, 2014, Larssen et al., 2005).

6. Conclusion

Four Late Palaeozoic intervals have been mapped on the Loppa High. The oldest interval (Int1) is a mix of carbonate and siliciclastic sediments, deposited at a tectonically active Late Carboniferous time on the Loppa High. An overlying interval (Int2) created primarily by evaporite precipitation has probably been deposited in a spill-out system, with interbedded carbonate successions. The following interval (Int3) is recognised as being of Permian age and consists mainly of carbonates deposited at various depths. Carbonate build-ups recognised in the middle of Int3 are vertically extending to the top of the interval and are associated with a catch-up carbonate system. The youngest interval (Int4) is a carbonate succession deposited at the end of Late Permian time, consisting of minimum the Røye Formation. The interval is characterized by a middle shelf carbonate succession and contain some build-up features that extend from Int3. Three build-up features have been mapped with a ring-shaped upper rim, which is recognised as an atoll like feature. An atoll is a clear sign of a lowstand and is therefore considered an important characteristic in the carbonate stratigraphic method.

The paleogeography of Loppa High is at the onset of the depositional phase of Int1 seen as a low angle ramp (less than 5°). Some extensional tectonic movement is believed to create further eastward tilting during the deposition of Int1. The tectonic movement is thought to have created internal sub-basins, valleys and highs on the Loppa High by the end of the depositional phase of Int1. The evaporite interval is further believed to be deposited in sub-basin locations during a time span from possibly Kasimovian – Early Sakmarian associated with high frequency and high amplitude eustatic sea level change driven by icehouse conditions on the earths southern hemisphere. At times with seasonally lowstand sea level conditions the ocean in the Loppa High region is believed to have been isolated from the larger ocean. The somewhat shallow sub-basins of the Loppa High were then evaporated, which created evaporite precipitation. These lowstand conditions created subaerial exposure and erosion of the uplifted Loppa High. Further uplift phases continued and the largest tectonic uplift and erosion phase is recognised in Late Permian time and resulted in a paleo-structure somewhat similar to what can be observed in seismic sections today (Larssen et al. 2005).

References

- AHLBORD, M., STEMMERIK, L., & KALSTØ, T. K. 2014. 3D seismic analysis of Karstified interbedded carbonates and evaporites, Lower Permian Gipsdalen Group, Loppa High, southwestern Barents Sea. *Marine and Petroleum Geology*, 16-33.
- ALVES, T. M. 2016. Polygonal mounds in the Barents Sea reveal sustained organic productivity towards the P–T boundary. *Terra Nova*, 28, 50-59.
- ASQUITH G. B. & GIBSON C. R. 1982. Gamma Ray Logs: Chapter V. In: 3 (ed.) Basic Well Log Analysis for Geologists. 15-21.
- BEAUCHAMP, B. 1994. Permian climatic cooling in the Canadian Arctic. *Geological Society of America Special Papers*, 288, 229-246.
- BEAUCHAMP, B. & BAUD, A. 2002. Growth and demise of Permian biogenic chert along northwest Pangea: evidence for end-Permian collapse of thermohaline circulation. *Palaeogeography, Palaeoclimatology, Palaeoecology*, 184, 37-63.
- BOGGS, S. 2010. Principles of Sedimentology and Stratigraphy. In: 4 (ed.). *Pearson Educational International*, 3-27.
- BOSENCE, D. 2005. A genetic classification of carbonate platforms based on their basinal and tectonic settings in the Cenozoic. *Sedimentary Geology*, 175, 49-72.
- BOSENCE, D., CROSS, N. & HARDY, S. 1998. Architecture and depositional sequences of Tertiary fault-block carbonate platforms; an analysis from outcrop (Miocene, Gulf of Suez) and computer modelling. *Marine and Petroleum Geology*, 15, 203-221.
- BRACHERT, T. & STUECKRAD, O. 2002. Tectono- climatic evolution of a Neogene intramontane basin (Late Miocene Carboneras subbasin, southeast Spain): revelations from basin mapping and biofacies analysis. *Basin Research*, 14, 503-521.
- BROWN JR, L. & FISHER, W. 1977. Seismic-Stratigraphic Interpretation of Depositional Systems: Examples from Brazilian Rift and Pull-Apart Basins: Section 2. Application of Seismic Reflection Configuration to Stratigraphic Interpretation. *University of Texas at Austin*, 213-248.
- BUBB, J. & HATLELID, W. 1978. Seismic stratigraphy and global changes of sea level, part 10: seismic recognition of carbonate buildups. *AAPG Bulletin*, 62, 772-791.
- CARON, V., NELSON, C. S. & KAMP, P. J. 2004. Transgressive surfaces of erosion as sequence boundary markers in cool-water shelf carbonates. *Sedimentary Geology*, 164, 179-189.
- CGMW. 2012. Standard Color Codes for the Geological Time Scale [Online]. <https://engineering.purdue.edu/Stratigraphy/charts/rgb.html>.
- CROSS, N., PURSER, B. & BOSENCE, D. 1998. The tectono-sedimentary evolution of a rift margin carbonate platform: Abu Shaar, Gulf of Suez, Egypt. *Sedimentation and Tectonics in Rift Basins Red Sea:-Gulf of Aden. Springer Netherlands, Norwegian Petroleum Society*, 271-272.
- DI LUCIA, M. S., JHOSNELLA; MUTTI, MARIA; COTTI, AXUM; BROBERG, KJETIL; SITTA, ANDREA 2011. Facie and seismic analysis from the Late Carboniferous - Early Permian Finnmark carbonate platform (southern Norwegian Barents Sea): A new assessment of the carbonate factories and depositional geometry. *American association of petroleum geology, AAPG Bulletin*, 62-109.
- EHRENBERG, S. N., NIELSEN, E., SVÅNÅ, T. & STEMMERIK, L. 1998. Depositional evolution of the Finnmark carbonate platform, Barents Sea: results from wells 7128/6-1 and 7128/4-1. *Norsk Geologisk Tidsskrift*, 78, 185-224.
- ELVEBAKK, G., HUNT, D. W. & STEMMERIK, L. 2002. From isolated buildups to buildup

- osaics: 3D seismic sheds new light on Upper Carboniferous–Permian fault controlled carbonate buildups, *Norwegian Barents Sea. Sedimentary Geology*, 152, 7-17.
- FALEIDE, J. I., VÅGNES, E. & GUDLAUGSSON, S. T. 1993. Late Mesozoic-Cenozoic evolution of the south-western Barents Sea in a regional rift-shear tectonic setting. *Marine and Petroleum Geology*, 10, 186-214.
- FORD, D. & WILLIAMS, P. D. 2013. Karst hydrogeology and geomorphology, John Wiley & Sons. *University of Auckland, New Zealand*, 271-321.
- GABRIELSEN, R. H., FÆRSETH, R. B., JENSEN, L. N., KALHEIM, J. E. & RIIS, F. 1990. NPD-Bulletin no 6, Structural elements of the Norwegian continental shelf. Part 1: The Barents Sea. *Ojledirektoratet*, 1-33.
- GUDLAUGSSON, S. T., FALEIDE, J. I., JOHANSEN, S. E. & BREIVIK, A. J. 1998. Late Palaeozoic structural development of the south-western Barents Sea. *Marine and Petroleum Geology*, 15, 73-102.
- HAQ, B. U. & SCHUTTER, S. R. 2008. A chronology of Paleozoic sea-level changes. *Science*, 322, 64-68.
- HERRON, D. A. & LATIMER, R. B. 2011. First steps in seismic interpretation. Society of *Exploration Geophysicists*, 153-163.
- HOLTE, H. V. 2016. Using Sequence Stratigraphy to Recognise Sea Level Change from Depositional Trends. *NTNU*, 1-49.
- JOHANSEN, S. E., Gudlaugsson, S. T., SVÅNÅ, T. A. & FALEIDE, J. I. 1994. Late Palaeozoic evolution of the Loppa High, Barents Sea. Geological Evolution of the Barents Sea, with Special Emphasis on the Late Palaeozoic Development, 1-25.
- KENDALL, C. G. S. C., BOWEN, B., ALSHARHAN, A., CHEONG, D.-K. & STOUT, D. 1991. Eustatic controls on carbonate facies in reservoirs, and seals associated with Mesozoic hydrocarbon fields of the Arabian Gulf and the Gulf of Mexico. *Marine Geology*, 102, 215-238.
- KENDALL, C. G. S. C. & SCHLAGER, W. 1981. Carbonates and relative changes in sea level. *Marine Geology*, 44, 181-212.
- LANDRØ, M. 2011. Seismic Data Acquisition and Imaging. Trondheim, 1-102.
- LARSEN, G., ELVEBAKK, G., HENRIKSEN, L. B., KRISTENSEN, S., NILSSON, I., SAMUELSBERG, T. A., SVÅNÅ, T., STEMMERIK, L. & WORSLEY, D. 2002. Upper Palaeozoic lithostratigraphy of the Southern Norwegian Barents Sea. *Norwegian Petroleum Directorate Bulletin*, 9, 76.
- LARSEN, G., ELVEBAKK, G., HENRIKSEN, L. B., KRISTENSEN, S., NILSSON, I., SAMUELSBERG, T. A., STEMMERIK, L. & WORSLEY, D. 2005. Upper Paleozoic lithostratigraphy of the southern Norwegian Barents Sea. Norsk Geologisk Undersøkelser, Bulletin, 444. *Geological Survey of Norway, Trondheim*, 3-40.
- LUNDIN NORWAY. 2016. Betydelig olje- og gassfunn i Barentshavet [Online]. <http://lundin-norway.no/betydelig-olje-og-gassfunn-i-barentshavet/>.
- MACINTYRE, I. G., BURKE, R. & STRICKENRATH, R. 1977. Thickest recorded Holocene reef section, Isla Perez core hole, Alacran Reef, Mexico. *Geology*, 5, 749-754.
- MITCHUM JR, R., VAIL, P. & SANGREE, J. 1977. Seismic stratigraphy and global changes of sea level: Part 6. Stratigraphic interpretation of seismic reflection patterns in depositional sequences: Section 2. Application of seismic reflection configuration to stratigraphic interpretation. *Exxon Production Research*, 117-133.
- NIELSEN, J. K., BŁAŻEJOWSKI, B., GIESZCZ, P. & NIELSEN, J. K. 2013. Carbon and Oxygen isotope records of Permian brachiopods from relatively low and high palaeolatitudes: climatic seasonality and evaporation. *Geological Society, London, Special Publications*, 376(1), 387-406.

- NILSSON, I. 2001. The geological evolution of Biørn a, Arctic Norway: implications for the Barents Shelf. *Norsk Geologisk Tidsskrift*, 81, 195-234.
- NPD. 2014. Lithostratigraphic chart Norwegian Barents Sea [Online] <http://www.npd.no/Global/Engelsk/2-Topics/Geology/Lithostratigraphy/BH-OD1409003.pdf>
- NPD FACT PAGES. 2016. NPD Fact Pages [Online]. <http://factpages.npd.no/>.
- POSAMENTIER, H. 1988. Eustatic controls on clastic deposition II—sequence and systems tract models. *Exxon Production Research Company*, 125-154.
- PURSER, B., BARRIER, P., MONTENAT, C., ORSZAG-SPERBER, F., D'ESTEVOU, P. O., PLAZIAT, J.-C. & PHILOBOS, E. 1998. Carbonate and siliciclastic sedimentation in an active tectonic setting: Miocene of the north-western Red Sea rift, Egypt. Sedimentation and Tectonics in Rift Basins Red Sea:-Gulf of Aden. *Springer Netherlands, Norwegian Petroleum Society*, 139-140.
- PURSER, B. H. & BOSENCE, D. 2012. Sedimentation and Tectonics in Rift Basins Red Sea:-Gulf of Aden, *Springer Netherlands, Science & Business Media*, 321-441.
- RAFAELSEN, B., ELVEBAKK, G., ANDREASSEN, K., STEMMERIK, L., COLPAERT, A. & SAMUELSBERG, T. J. 2008. From detached to attached carbonate buildup complexes—3D seismic data from the upper Palaeozoic, Finnmark Platform, southwestern Barents Sea. *Sedimentary Geology*, 206, 17-32.
- RUIZ- ORTIZ, P., BOSENCE, D., REY, J., NIETO, L., CASTRO, J. & MOLINA, J. 2004. Tectonic control of facies architecture, sequence stratigraphy and drowning of a Liassic carbonate platform (Betic Cordillera, Southern Spain). *Basin Research*, 16, 235-257.
- SARG, J. 1988. Carbonate sequence stratigraphy. *Exxon Production Research Company*, 155-181.
- SAYAGO, J., DI LUCIA, M., MUTTI, M., COTTI, A., SITTA, A., BROBERG, K., PRZYBYLO, A., BUONAGURO, R. & ZIMINA, O. 2012. Characterization of a deeply buried paleokarst terrain in the Loppa High using core data and multiattribute seismic facies classification. *AAPG bulletin*, 96, 1843-1866.
- SCHLAGER, W. 1981. The paradox of drowned reefs and carbonate platforms. *Geological Society of America Bulletin*, 92, 197-211.
- SCHLAGER, W. 1989. Drowning unconformities on carbonate platforms. Controls on carbonate platforms and basin development. *Society for Sedimentary Geology, SEPM special publications*, 44, 15-25.
- SCHLAGER, W. 1991. Depositional bias and environmental change—important factors in sequence stratigraphy. *Sedimentary Geology*, 70, 109-130.
- SCHLAGER, W. & PURKIS, S. J. 2013. . Bucket structure in carbonate accumulations of the Maldive, Chagos and Laccadive archipelagos. *International Journal of Earth Sciences*, 102(8), 2225-2238.
- SHERIFF, R. E. & GELDART, L. P. 1995. Exploration Seismology. *Cambridge University Press*, 349-420.
- SMELROR, M., PETROV, O., LARSSSEN, G. B. & WERNER, S. 2009. Geological history of the Barents Sea. *Norges Geologiske Undersøkelse*, 1-135.
- SOREGHAN, G. S. & GILES, K. A. 1999. Amplitudes of late Pennsylvanian glacioeustasy. *Geology*, 27, 255-258.
- STEMMERIK, L. & WORSLEY, D. 1989. Late Palaeozoic sequence correlations, North Greenland, Svalbard and the Barents Shelf. Correlation in hydrocarbon exploration. *Springer Netherlands, Norwegian Petroleum Society*, 99-111.
- STEMMERIK, L. 1997. Permian (Artinskian Kazanian) Cool-Water Carbonates in North Greenland, Svalbard and the Western Barents Sea. *Society for Sedimentary Geology, SEPM*, 244-364.
- STEMMERIK, L., ELVEBAKK, G. & WORSLEY, D. 1999. Upper palaeolithic carbonate reservoirs

- in the norwegian arctic shelf: upper palaeolithic carbonate reservoirs in the norwegian arctic shelf. *Petroleum Geoscience*, 5, 173-187.
- STEMMERIK, L. & WORSLEY, D. 2000. Upper Carboniferous cyclic shelf deposits, Kapp Kåre Formation, Bjørnøya, Svalbard: response to high frequency, high amplitude sea level fluctuations and local tectonism. *Polar Research*, 19, 227-249.
- STEMMERIK, L. & WORSLEY, D. 2005. 30 years on-Arctic Upper Palaeozoic stratigraphy, depositional evolution and hydrocarbon prospectivity. *Norwegian Journal of Geology/Norsk Geologisk Forening*, 85, 151-168.
- STEMMERIK, L. 2008. Influence of late Paleozoic Gondwana glaciations on the depositional evolution of the northern Pangean shelf, North Greenland, Svalbard, and the Barents Sea. *Geological Society of America Special Papers*, 441, 205-217.
- VAIL, P. R. 1987. Seismic stratigraphy interpretation using sequence stratigraphy: Part 1: Seismic stratigraphy interpretation procedure. *Rich University*, 1-10.
- VAIL, P. R., HARDENBOL, J. & TODD, R. G. 1984. Jurassic unconformities, chronostratigraphy, and sea-level changes from seismic stratigraphy and biostratigraphy. *Exxon Production Research Company*, 129-144.
- VAN WAGONER, J. C., MITCHUM, R., CAMPION, K. & RAHMANIAN, V. 1990. Siliciclastic sequence stratigraphy in well logs, cores, and outcrops: concepts for high-resolution correlation of time and facies. *The American Association of Petroleum Geology*, 7, 1-55.
- WRIGHT, V. 1992. Speculations on the controls on cyclic peritidal carbonates: ice-house versus greenhouse eustatic controls. *Sedimentary Geology*, 76, 1-5.
- ZIEGLER, P. A. 1982. Geological Atlas of Western and Central Europe. *Amsterdam, Shell International Petroleum*, 15-75.